Co-pyrolysis of coal and raw/torrefied biomass: A review on chemistry, kinetics and implementation

Saartjie M. Gouws, Marion Carrier, John Reginald Bunt, Hein W.J.P. Neomagus

Co-pyrolysis of coal and raw/torrefied biomass: A review on chemistry, kinetics and implementation

S.M. Gouws [a], M. Carrier [b], J.R. Bunt [a,*], H.W.J.P. Neomagus [a]

[a] Center of Excellence in Carbon-based Fuels, School of Chemical and Minerals Engineering, North West-University, Potchefstroom, 2520, South Africa
[b] RAPSODEE, CNRS UMR 5203, Université de Toulouse, IMT Mines Albi, Campus Jarlard, 81013, Albi CT Cedex 09, France

Keywords:
Co-pyrolysis
Biomass
Coal
Torrefaction
Chemistry
Kinetics

A B S T R A C T

Thermochemical conversion via co-pyrolysis has the potential to be an efficient route for converting biomass to bio-energy and bio-refinery products. In this review, the implementation of co-pyrolysis of torrefied biomass and coal was critically assessed against co-pyrolysis of raw biomass and coal from both a fundamental and engineering perspective. This evaluation showed fundamental advantages for torrefaction of biomass prior to co-pyrolysis such as a decrease in mass and heat transfer limitations due to an increase in permeability and thermal conductivity of biomass. Co-pyrolysis volatiles may also be upgraded through the catalytic activity of the torrefied biomass surface, producing higher quality oil. Due to properties more similar to coal, torrefied biomass requires less energy for milling (lower operating costs) and can be more easily blended with coal in reactor feeding systems. A state-of-the-art research on co-pyrolysis kinetics revealed that reactivities of blends may be predicted from kinetic parameters of individual feedstocks using an additive approach. To conclude on the preferred reactor design for this process, different reactors were evaluated based on heat transfer mode, operation and product formation. Although both the fluidized bed and rotating cone reactor provide high oil yields, the rotating cone has been more successful commercially. This design shows great promise for specifically co-pyrolysis due to the intimate contact that may be achieved between fuels to maximize synergy. The co-pyrolysis of torrefied biomass and coal may be encouraged from a scientific point of view, however further research is recommended on the effective integration of torrefaction and co-pyrolysis technologies.

1. Introduction

The production of affordable, sustainable and clean energy is a cornerstone for global socio-economic growth [1]. The total world energy consumption is expected to rise a further 28% by 2040 [2]. Fossil fuels are a widely available energy source, however this source of energy production is associated with large amounts of greenhouse gas (GHG) emissions, a driver of climate change [3]. At COP25 2019, the urgency for countries to improve their emission reduction strategies was highlighted.

Considering the need that faces governmental agencies to decrease GHG emissions, quick implementation of mature green technologies is required. Technologies utilizing fossil fuels such as coal are well established, however one of the important contributions to GHG reduction from industry is the shift towards renewable feedstocks [4]. Patel and co-workers [3] recently reviewed the techno-economic and life cycle assessment of thermochemical conversion technologies and suggested that the implementation of biomass primarily depends on the cost competitiveness of biomass-based energy and chemicals compared to those derived from fossil fuels. They concluded that the cost of bioenergy-based technologies remains higher.

To stimulate the transition to bioenergy-based technologies, a reduction in process costs is required. This may be achieved by improving the efficiency of these technologies regarding energy and chemical production and GHG abatement [5]. To improve the existing industrial technology, a thorough understanding of thermochemical conversion processes is required. The pyrolysis process is the starting point of all these technologies, however stand-alone pyrolysis technology has also attracted wide attention [6]. This technology is being extensively developed in the bioenergy area for significant potential to co-generate energy and chemicals [7].

The scientific and industrial community's interest in the pyrolysis process has increased significantly over the past few decades. The amount of scientific documents published on pyrolysis using either coal or biomass as feedstock for different years is shown in Fig. 1. It can be

* Corresponding author.
E-mail address: John.Bunt@nwu.ac.za (J.R. Bunt).

List of abbreviations

AAEM	Alkali and alkaline earth metals
BET	Brunauer–Emmett–Teller
COP25	25th United Nations Climate Change Conference
CPD	Chemical percolation devolatilization
DAEM	Distributed activation energy model
DSC	Differential scanning calorimetry
DTG	Derivative thermogravimetric
FTIR	Fourier transform infrared spectroscopy
GC	Gas chromatography
GC-MS	Gas chromatography mass spectrometry
GHG	Greenhouse gas
HPLC	High performance liquid chromatography
NMR	Nuclear magnetic resonance
PAH's	Polyaromatic hydrocarbons
SEM	Scanning electron microscope
TGA	Thermal gravimetric analysis

observed that research in both coal and biomass pyrolysis processes has increased significantly since the 1960s. The oil crises in the 1970s have intensified development in these areas, however since the late 1990s an exponential shift towards biomass pyrolysis research is evident with the signatures of conventions and protocols (Fig. 2). The increased awareness of environmental issues related to fossil fuel usage in the twenty first century and resulting calls for clean and renewable energy sources is the main reason for the observed shift in scientific interest [8]. Research in coal pyrolysis has become less popular compared to biomass pyrolysis in the twenty first century, however an increase is still evident in countries with high coal reserves such as China [9].

A viable option for industrial thermochemical conversion technologies to transition to renewable feedstocks is the co-utilization of lignocellulosic biomasses with coal as feedstock in existing coal-based processes [11,12]. For pyrolysis technologies, in particular, the co-utilization of biomass and coal has become an attractive option not merely due to a reduction in the carbon footprint of the overall process [13], but also due to the potential of producing higher oil yields with improved quality (composition closer resembling crude-oil) [14].

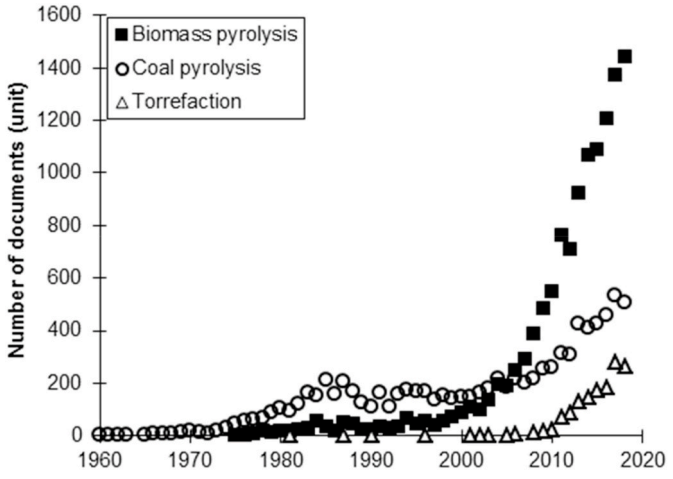

Fig. 1. Increase of scientific publications on pyrolysis research using either coal (Scopus keywords: Pyrolysis AND coal) or biomass (Scopus keywords: Pyrolysis AND biomass) as feedstock and torrefaction (Scopus keywords: Torrefaction) – Access on January 14, 2020.

During co-pyrolysis, the hydrogen released from biomass stabilizes the large radicals produced from coal resulting in improved oil quality and yields [15] (See Section 3 for further details). Several authors have reviewed co-pyrolysis of biomass and coal along with other feedstocks such as waste plastics and tyres [6,16–18]. The thermal decomposition of materials was broadly discussed in these reviews, but no information on co-pyrolysis kinetic studies were reported. Abnisa and co-workers [6] concluded that the success of the co-pyrolysis process mainly lies with the synergistic effect observed during the reaction between different materials which increases the yield and quality of the oils. They suggested that the pyrolysis reactor configuration is important for achieving synergistic/antagonist effects; however, the review lacked a detailed comparison between different technologies.

Although the co-pyrolysis of biomass and coal is favourable to upgrade the quality of the oil products through synergistic effects, large amounts of oxygenated species mostly derived from the biomass are present in the oil [19]. Due to its high oxygen content, bio-oil has an acidic nature and a high chemical reactivity, which results in phase separation during storage [20].

Biomass pre-treatment techniques enable the optimization of pyrolysis product yields and composition, and limit the formation of undesired products [21]. Pre-treatment techniques have been comprehensively reviewed (see Section 4.1). Among these pre-treatment methods torrefaction is considered one of the most promising [22]. This is evident from the increasing trend in scientific publications on torrefaction (Fig. 1). This mild pyrolysis treatment is performed at temperatures of 200–300 °C resulting in moisture removal, the decomposition of hemicelluloses and partial depolymerisation of lignin and cellulose [23]. The physical and chemical properties of biomass as fuel are improved by increasing its energy density, lowering O/C and H/C ratios and inverting its hydrophilic nature [24].

The use of torrefied biomass as feedstock for the pyrolysis process also improves the quality of the resulting bio-oil by reducing the moisture, oxygen and acid content, and increasing the carbon content [20]. This process has developed rapidly but has only been reviewed recently [25,26]. Both these reviews focused on the effects of torrefaction on the quality of the pyrolysis products, and demonstrated the potential to upgrade bio-oil quality but at the cost of bio-oil yield. Dai and co-workers [26] analysed the integrated process of torrefaction and pyrolysis and concluded that the process is cost-effective with good economic potential. It was suggested that the integration of torrefaction with advanced pyrolysis techniques such as co-pyrolysis can result in an increased competitiveness of commercial bio-oil.

The co-pyrolysis of torrefied biomass and coal combines the advantages of co-utilization of biomass and coal with the advantages of torrefied biomass as feedstock in pyrolysis technologies. Reviews on co-pyrolysis studies by Abnisa et al. [6], Quan and Gao [16], Hassan et al. [17] and Mushtaq et al. [18] have mainly focused on summarizing general trends, which do not convey clear conclusions on the origins of antagonist/synergistic events due to a disjoint approach to evaluate the different scales of pyrolysis. The novelty of this review is the fundamental evaluation of chemical and physical aspects of the co-pyrolysis process, which has been neglected in other reviews. To the authors' knowledge, this is also the first review providing insights into fundamental differences in the co-pyrolysis of torrefied biomass and coal compared to co-pyrolysis of raw biomass and coal. For co-pyrolysis studies using raw/torrefied biomass and coal, only 3% of studies have included torrefied material. The recent progress made in the understanding of chemistry and physics covering mainly mechanistic pyrolysis aspects (Sections 3.1 and 3.2) are first reviewed followed by a state-of-the-art on kinetics of co-pyrolysis (Section 3.3). The engineering applications of this process are then discussed in Section 4. Finally, the conclusions and prospects are summarized in Section 5.

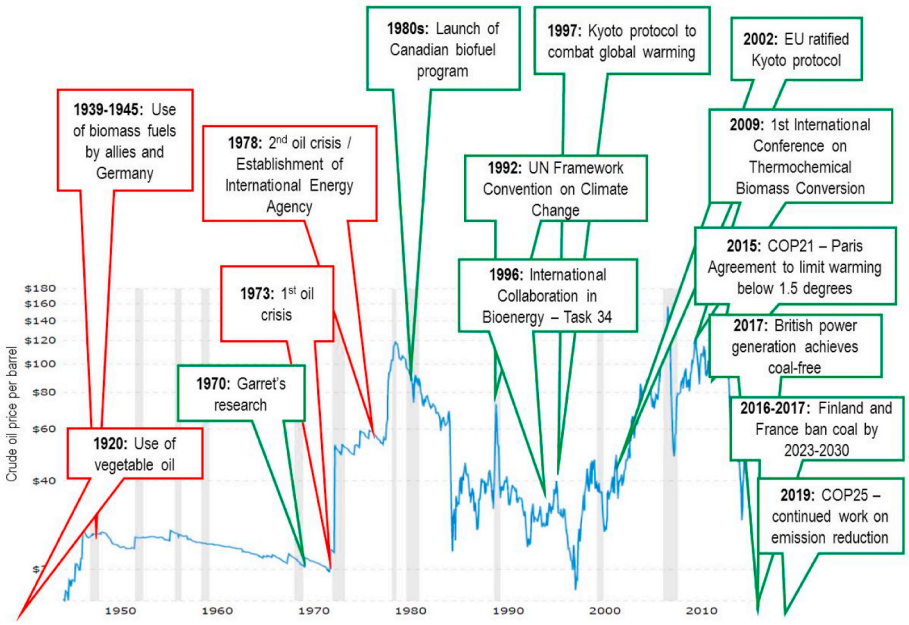

Fig. 2. Historical events that allowed the deployment of biofuels' research activities [10]. Red textboxes represent geopolitical reasons (wars, economic crisis) that largely explained the shifts in the demand for crude oil and green textboxes represent different actions that countries undertook to announce the imminent phase-out of coal-fired power plants. (For interpretation of the references to colour in this figure legend, the reader is referred to the Web version of this article.)

2. Feedstock origin

2.1. Feedstocks: coal and biomass

The composition of the most popular studied types of biomass and coal are shown in Table 1 and reveal important chemical differences. Lignocellulose is described as a polymeric structure made up by three main constituents (i.e. cellulose, hemicelluloses, lignin). The chemical and structural properties of a specific biomass mainly depend on the content and nature of these biopolymers [27]. On the other hand, coal consists of small "nuclei" of aromatic and naphthenic rings, which are linked to each other by bridges of aliphatic chains or heteroatoms [28]. The high aromaticity of coal is reflected in its high content of C and low content of H [29].

General correlations between physico-chemical properties of biomass and coal can be used as a predictive tool to determine the suitability of the feedstock for a certain application and different reviews have summarized these correlations [30,31]. For the co-processing of torrefied biomass and coal, correlations based on the ultimate analysis of the feedstock are likely to be the best choice for a predictive tool due to a more accurate estimation of the reactants ratio [30].

2.2. Thermal behaviour of feedstocks

Thermogravimetric measurements are conventionally used to assess thermal behaviour and organic composition of feedstocks [54–56].

Table 1
Proximate and ultimate analyses, CV value and molar O/C and H/C ratios of different types of biomasses and coals of different ranks.

Feedstock	Proximate analysis (wt% d.b.)[a]			Ultimate analysis (wt% d.a.f)[b]					CV (d.b.) (MJ kg^{-1})[c]	O/C[d]	H/C[e]	Ref.
	VM[f]	FC[g]	Ash	C	H	N	O	S				
Biomass												
Softwood												
Pine chips	72.4–87.0	12.6–21.6	0.3–6.0	46.1–52.8	5.3–6.1	0.1–0.5	40.5–48.4	<0.3	19.0–19.8	0.6–0.8	1.2–1.6	[32–36]
Hardwood												
Sawdust	84.6–91.3	14.3–19.6	0.1–1.1	45.3–52.0	6.0–6.1	0.2–0.6	41.6–47.1	0.1–1.1	17.7–20.4	0.7–0.8	1.4–1.6	[35–39]
Grass												
Switchgrass	76.7–80.4	14.4–14.5	5.1–8.9	39.7–49.7	4.9–6.1	0.6–0.7	31.8–43.4	<0.2	12.6–18.1	0.6–0.7	1.2–1.8	[37,40]
Straw												
Rice straw	71.6–88.7	8.1–14.5	8.9–13.9	43.6–45.4	5.3–7.4	0.4–0.8	33.0–50.6	<0.1	16.2–18.9	0.5–0.8	1.4–2.0	[40–43]
Coal												
Peat	61.2–78.9	10.0–24.3	6.5–18.8	50.5–56.4	5.4–6.0	1.4–2.5	35.7–41.2	0.5–0.9	17.4–22.4	0.3–0.5	1.1–1.3	[44–46]
Lignite	38.0–54.4	36.3–50.0	9.4–33.3	66.8–73.2	4.5–5.1	1.0–2.0	16.4–22.0	1.3–2.0	26.5–31.7	0.1–0.2	0.7–1.1	[44,47,48]
Bituminous	20.0–26.9	54.8–55.8	18.3–35.0	78.8–82.9	4.3–5.0	1.6–2.0	10.0–15.1	0.6–1.8	19.9–36.4	0.1–0.2	0.6–0.8	[44,49–51]
Anthracite	4.2–30.4	80.3–86.8	6.0–9.0	84.8–94.4	2.1–3.5	<1.4	1.7–6.2	<1	30.6–36.2	<0.1	0.3–0.5	[48,52,53]

[a] d.b. – dry basis.
[b] d.a.f. – dry ash free.
[c] CV – calorific value.
[d] O/C – oxygen to carbon molar ratio.
[e] H/C – hydrogen to carbon molar ratio.
[f] VM – volatile matter.
[g] FC – fixed carbon.

During thermal degradation of woody biomass, different stages can be identified in weight loss curves (Fig. 3): below 200 °C where the slight decay is due to drying and the release of light volatiles [57] and 200–500 °C where significant mass loss is observed. Hemicellulose is the most reactive component and decomposes in the range of 225–325 °C, cellulose in the range of 305–375 °C, while lignin degrades gradually in the range of 250–500° [58]. Compared to biomass, coal displays smaller mass losses. The first stage of thermal decomposition occurs below 400 °C corresponding to drying and the release of low molecular organic species [59]. The second stage includes the main devolatilization range between 400 and 600 °C.

The torrefaction pre-treatment technique applied to biomass upgrades the fuel characteristics to closer match those of coal. Compared with raw biomass, the mass loss curve of torrefied biomass shows a closer resemblance to the coal mass loss curve (Fig. 3), mainly due to the removal of hemicelluloses during torrefaction [60–62].

3. Fundamentals of co-pyrolysis

Co-pyrolysis of biomass and coal cannot be dissociated from the concept of synergistic/antagonist effects because it is expected to draw several advantages in terms of emissions, energy savings and enhancing product quality. Here, we would like to reflect on the current usage of the word 'synergistic' that is often mentioned when discussing chemical mechanisms in co-pyrolysis. The semantic of the word confirms that 'synergy' is used when the interaction of components when combined produce a greater effect than the sum of the individual components, suggesting a positive impact. In this review, we will use product yields as indicators for synergies and antagonisms. These effects are evident when the combined individual product yields (oil, gas and char) differ from the total sum. This approach is often referred to as the additive method. To be specific on the origin of experimental discrepancies, here we analyse how major parameters impact co-pyrolysis features. Past co-pyrolysis studies performed in different reactors and using thermogravimetric analysis were respectively collated in Tables 2 and 3. We would like to stress the fact that it is challenging to compare the outcomes of studies from Table 2 considering the variability between set-ups and characterization methodologies; thermogravimetric analysis being the most commonly applied thermoanalytical technique in solid-phase thermal degradation studies for obtaining kinetic data [64].

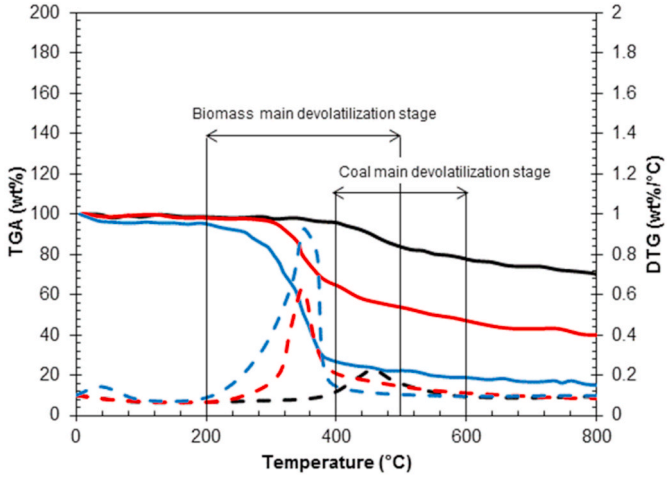

Fig. 3. TGA and DTG curves for coal (— coal TGA, — — coal DTG), torrefied wood (— torrefied biomass TGA, - - torrefied biomass DTG) and raw wood (— raw biomass TGA, - - raw biomass DTG) (adapted from Lu and co-workers [63]).

Table 2
Summary of process parameters for co-pyrolysis studies on different reactor setups.

Biomass/coal type	Coal	Biomass	Biomass blend ratios (wt%)	Reactor type	Capacity (g)	Gas Flow rate (mL/min)	Particle size (μm)	Heating rate (K/s)	Temperature (°C)	Pressure (bar)	Product characterization methodology	Ref.
	H/C molar ratio - AC (%, db[a])											
Silver birch, forest residue/Daw Mill, polish coal	0.70–4.7/ 0.77–10	1.60–1.9/ 1.37–2.1	50	Fluidized bed	0.05–0.1	He	106–150	NR[b]	850,1000	20	Liquids/gas: Set-up originally designed for studying char reactivity – no detailed description of total volatiles and oil collection Char: Reactivity measured by TGA	[65]
Corn cob/subbit.[c]	0.98–22.96	1.53–1.57	20/40/60/ 80	Fluidized bed	20	N_2, 7000	C: 600–1000, B: 1000-2000	NR	500–700	1	Gas: Collected in gas bags, analysed with GC Char: Not characterized Liquids: GC-MS analysis	[66]
JiaDuoBao/Lignite	0.8–16.8	1.6–6.4	10/20/40/ 50	Fluidized bed	0.02	Ar, 300	150–180	NR	600–850	1	Gas: Online analysis by MS, collected in gas bags, analysed with GC Char: Not characterized Liquids: Not characterized	[67]
Sawdust/Drayton coal	0.8–15.8	1.3–0.4	5/10	Drop tube	3	N_2, 500	C: 45–63, B: 9-125	10^4	900–1400	1	Gas: Online analysis by fast response GC Char: XRF analysis Liquids: Not characterized	[68]
Sawdust/bit.[d]	0.83–8.7	1.6–0.99	20/40/60/ 80	Drop tube	10	N_2, 500	180–250	NR	800–1400	1	Gas: Measured by flow meter, collected in bags, analysed by GC Char: Reactivity measured by TGA Liquids: Not characterized	[69]

(continued on next page)

Table 2 (*continued*)

Biomass/coal type	Coal	Biomass	Biomass blend ratios (wt%)	Reactor type	Capacity (g)	Gas Flow rate (mL/min)	Particle size (μm)	Heating rate (K/s)	Temperature (°C)	Pressure (bar)	Product characterization methodology	Ref.
	H/C molar ratio - AC (%, db[a])											
Legume straw/lignite	0.8–11.0	1.6–1.8	0–100	Drop tube	NR	N_2, 35	300–450	NR	500–700	1	Gas: Analysed with GC Char: Reactivity determined in fixed bed	[70]
Cellulose, hemicellulose, lignin/bit.	0.7–16.1	1.7–0.07/ 1.7–3.8/ 1.0–3.7	20/50/75	Drop tube	1	N_2, 100	NR	NR	600–1000	1	Gas: Collected in gas bags, analysed with GC Char: Not characterized Liquids: Not characterized	[71]
Pine sawdust, legume straw/brown, bit.	0.8–11.0/ 0.7–17.5	1.6–0.3/ 1.6–0.3/ 1.6–1.7	0–100	Drop tube	4–6	N_2, 35	300–450	8.3	500–700	1	Gas: Collected in gas bags, analysed with GC Char: Char reactivity determined in fixed bed Liquids: Analysed by SEC, GC-MS	[72]
Pine/subbit.	0.79–5.71	1.59–0.34	0–100	Drop tube	NR	N_2	C: 300–450, B: 450-900	NR	600	1	Gas: Collected in gas bags, analysed with GC Char: Not characterized Liquids: Not characterized	[73]
Switchgrass/bit.	0.90–11.41	1.6–9.1	15/30/50	Semi-batch drop tube	1	Ar, 2000	297–1190	NR	900	1	Gas: Collected in bags, analysed by GC-MS, online MS. Char: Ash elemental analysis via ICP OES, ultimate analysis Liquids: GC-MS analysis, ultimate analysis	[13]
Rice straw/bit.	0.86–6.57	1.7–13.9	20/50/80	Semi-batch drop tube	0.3	Ar, 500	C: 125-180 B:250-420	10^3–10^4	600–1200	1	Gas: Collected in gas collector, analysed with GC Char: Analysis by XRD, SEM, surface area, pore size distribution (BET), char reactivity by TGA Liquids: Not characterized	[74]
Wood, rice straw/ subbit.	1.1–9.6	1.8–2.8/ 1.8–12.0	25/50/75	Semi-batch drop tube	4	N_2, 120	150–250	NR	800	1	Gas: Collected in gas bags, analysed with TCD-GC Char: Analysis by SEM, surface area and pore size distribution (BET) Liquids: GC-MS analysis	[75]
Pine/subbit, lignite	0.76–6.6 0.8–25.7	1.4–0.6	10/20/50	Semi-batch drop tube	0.1	Ar, 4500	106–300	400–1000	600–925	1	Gas: Collected in bags, analysed by GC-MS, online MS. Char: Not characterized Liquids: GC-MS analysis	[15]
Wood/lignite	0.8–24.3	1.5–0.8	30/50/70	Semi-batch drop tube	NR	N_2, 100	<74	NR	600–1000	1	Gas: Collected in gas bags, analysed with GC Char: Analysed using SEM Liquids: Not characterized	[20]
Sugar beet/lignite	0.81–5.8	1.73–3.0	50	Semi-batch drop tube	1 pellet	Ar, 4500	Pellets Φ~13 mm	NR	600	1	Gas: Not characterized Char: Proximate, ultimate analysis Liquids: Not characterized	[76]
Corn stalk/subbit.	0.7–3.4	1.5–5.7	10/30/50/ 70/90	Moving bed pyrolyzer	100	None	C: <4000 B: Pellets (2000 × 6000)	NR	700–800	1	Gas: Collected in gas bags, analysed with GC Char: Ultimate analysis, ash melting point, XRF Liquids: Not characterized	[77]
Silver birch, forest residue/Daw Mill, Polish coal	0.70–4.7 0.77–10	1.60–1.9 1.37–2.1	33/49/52/ 73	Hot rod FB	0.05	N_2, 100	106–150	10	850,1000	1,5,10,20	Liquids/Gas: Set-up originally designed for studying char reactivity – no detailed description of total volatiles and tar collection Char: Reactivity measured by TGA	[65]

(*continued on next page*)

Table 2 (*continued*)

Biomass/coal type	Coal	Biomass	Biomass blend ratios (wt%)	Reactor type	Capacity (g)	Gas Flow rate (mL/min)	Particle size (μm)	Heating rate (K/s)	Temperature (°C)	Pressure (bar)	Product characterization methodology	Ref.
	H/C molar ratio - AC (%, db[a])											
Sawdust/bit.	0.83–8.7	1.6–0.99	20/40/60/80	Fixed bed	10	N_2, 500	180–250	NR	800–1400	1	Gas: Measured by flow meter, collected in bags, analysed by GC Char: Reactivity measured by TGA Liquids: Not characterized	[69]
Sawdust/lignite	0.97–10.3	1.59–1.69	20/50/80	Fixed bed	2	N_2, 100	C:150-500 B:<125	NR	400–900	1	Gas: Collected in bags, analysed by GC Char: Analysed by IR spectra Liquids: Analysed by GC-MS	[78]
Corn cobs, corn stover, bagasse/bit.	0.8–38.6	1.6–1.6, 1.7–24.5, 1.6–10.3	5/27.5/50	Fixed bed	300–600	N_2, 2000	C: 6700–20000, B: 50-20000	0.2–0.25	400–600	1–26	Gas: Collected in bags, analysed by GC Char: Not characterized Liquids: Analysed by GC-MS	[79]
Rice straw/bit.	0.85–6.9	1.96–11.01	20/40/60/80	Fixed bed	15	N_2, 500	180–250	NR	700–900	1	Gas: Measured by flow meter, collected in bags, analysed by GC Char: Analysed by SEM, proximate and ultimate analyses Liquids: Condensed, analysed by GC-MS	[43]
Straw/lignite	1.1–10.8	1.9–9.73	50	Fixed bed	30	N_2, 100	<177	0.3	500–550	1	Gas: Measured by flow meter, collected in bags, analysed by GC Char: Raman, XPS analysis Liquids: Condensed and analysed by GC-MS	[80]
Sawdust/subbit.	0.68–7.43	1.57–0.76	20/40/60/80	Fixed bed	20	N_2, ~25000	<1000	NR	500–700	1	Gas: Collected in bags and analysed by GC and IR analyser Char: Not characterized Liquids: Not characterized	[81]
Rice husk/lignite	0.9–5.4	1.6–15.9	50	Vacuum Fixed bed	10	N_2	130–180	0.2	900	−0.75 (vacuum)	Gas: Collected in bags, analysed by GC Char: Analysed for surface area (BET) Liquids: Analysed by GC-MS	[82]
Corncob/lignite	0.7–9.4	0.9–2.0	33/50/67	Two-stage fixed bed	3	None	125–154	0.17	1000	1	Gas: Online analysis by MS Char: Reactivity measured by TGA, Raman spectra, surface area (BET) Liquids: Not characterized	[83]
Sawdust/Drayton coal	0.8–15.8	1.3–0.4	5/10/25/50	Horizontal tubular	1	N_2, 50	C: 45-63 B: 9-125	0.2–0.8	200–1400	1	Gas: Online analysis by fast response GC Char: Not characterized Liquids: Not characterized	[84]
Safflower seed/lignite	1.1–44.6	1.8–2.3	3/5/7/10/33/50	Fixed bed	10	N_2, 100	C: 500–1000, B: 600-850	0.1	450–700	1	Gas: Not characterized Char: Not characterized Liquids: Elemental analysis, calorific value, FTIR, GC-MS, ^{1}H NMR	[85]

[a] d.b. – dry basis.
[b] NR – not reported.
[c] Subbit. – subbituminous.
[d] bit. – bituminous.

Table 3
Summary of process parameters for co-pyrolysis thermogravimetric studies.

Biomass/coal type	Biomass(es)	Coal(s)	Blend ratios (Biomass wt %)	Capacity (mg)	Gas flow (mL/min)	Particle size (μm)	Heating rate (°C/min)	Temperature (°C)	Pressure (bar)	Ref.
	H/C molar ratio - Ash (%, db[a])									
Pine chips/lig.[c]	1.4–1.0	1.1–68.7/ 0.9–34.3	20/60/80	nr[b]	Nr	750–1200	100	110–900	1	[87]
Pine sawdust/bit.	1.4–1.7/ 1.8–45.6	0.5–10.7/ 0.8–7.5	15–40	10–15	N_2 300	70–100	20	100–900	1	[88]
Olive kernel, forest- and cotton residue/lig.	1.4–2.6/ 0.5–2.1/ 1.4–0.2/ 1.5–6.6	1.2–13.0	5/10/20	20–25	N_2 45	<250	10	850	1	[89]
Olive kernel, forest- and cotton residue/lig.	1.4–2.6/ 1.4–2.1/ 1.4–0.2/ 1.5–6.6	1.2–13.0	5/10/20	20/25	N_2 45	<75/ <250/ <450	10/100	to 110 & to 850	1	[90]
Wood waste, wheat straw/subbit.[d]	1.3–0.1/ 1.5–3.3	0.7–9.7	50/70/80/ 90	100	Ar 50	nr	20	to 1300	1	[91]
Pinewood/lig, bit.[e]	1.3–2.4	1.3–11.0/ 0.8–3.4/ 0.9–5.0	25/50/75	15	N_2 nr	75–90	25	to 900	1	[19]
Pine, pellets, olive residue, hazelnut shells, paper sludge/bit	1.4–1.7/ 1.5–2.3/ 1.6–1.2/ 1.3–1.3/ 1.7–47.0	0.8–13.8	15/40	15	N_2 60	125–300	20	105 to 1000	1	[92]
Safflower seed/lig.	1.8–2.3	1.1–44.6	33/50/66	25	N_2 40	500–1000	5	to 800	1	[85]
Corn cob/lig.	1.6–0.9	1.0–18.3	10/50/90	nr	He 50	< 74	10	to 600	1	[93]
Wood waste/lig.	1.3–1.5	0.7–28.5	50/60/90	5	N_2 100	C: 149-210 B: 354-500	40	to 1000	1	[94]
sawdust/subbit., bit.	1.6–3.8	0.8–11.6/ 1.3–19.7	50	5	N_2 100	53–75	10/30/50	to 1200	1	[95]
Palm fruit bunches, kernel shell, mesocarp fibre/ lig.	1.6–4.5/ 1.5–10.2/ 1.3–10.5	1.2–5.8	20/40/50/ 60/80	20	N_2 nr	<212	10/20/40/ 60	to 900	1	[96]
Corn residue/lignite	1.6–7.6	0.8–12.5	10/20	5	He 100	nr	10/30/100	to 900	1	[97]
Hazelnut shell/ peat, lig., bit., anth.[f]	nr-4.3	nr-7.7/ nr-42.5/ nr-20.3/ nr-6.8/ nr-4.5	10	40–44	N_2 40	250	40	to 900	1	[98]
Sugar beet pulp/ lignite	1.7–3.0	0.8–5.8	50	10	N_2 50	74–149	20	to 900	1	[76]
sawdust/subbit.	1.6–0.8	0.7–7.4	40	<10	N_2 200	<250	15	to 900	1.2	[81]
Sawdust, rice straw/ lig.	1.4–1.6/ 1.1–11.8	0.7–31.3	20/50/70	10	N_2 70	74–149	10	to 1000	1	[99]
Sugarcane bagasse, corn cob/bit	1.6–10.3/ 1.6–1.6	0.8–38.6	10/20/40	5–25	N_2 150	< 212	5/10/50	to 900	1	[100]
C. vulgaris algae/ semi-anth	1.6–10.3	0.9–21.6	30/50/70	6	N_2 100	<200	10/20/40	to 1000	1	[101]
Japanese cedar chips/anth.	1.22–0.0	0.7–13.7	25/50/75	5	N_2 100	74–149	20	to 800	1	[63]
Wood chips, macadamia nut shells/bit.	1.3–1.2/ 1.3–0.2	1.0–23.6	80/85/90/ 95	10	N_2 20	250–350	5/10/15/20	to 1000	1	[59]
Pine chips/bit., subbit.	1.3–0.9	0.4–8.1/ 0.8–14.2	50/100	1000	N_2 3500	<125	1st stage: 10, 2nd stage: 10/20/30/ 40	1st stage: 105 °C, 2nd stage: to 1000 °C	1	[102]
Switchgrass, sawdust/sub.	1.6–6.3/ 1.5–0.4	0.7–30.5/ 0.3–2.0	25/50/75	5/10/15	N_2 250/ 500/ 750	300–355	25	to 800 °C	1–100	[103]
Pine/subbit.	1.6–0.3	0.8–5.7	25/50/75	10–15	N_2 nr	450-900/ 300-450	10	to 800	1	[73]
Fungi residue/bit.	0.7–12.4	0.7–15.4	25/50/75	10	N_2 60	<74	10/20/40	to 1200	1	[104]
Pine sawdust/lig.	1.6–1.7	1.0–10.3	20/50/80	~10	N_2 80	150–500 and <125	10	to 1000	1	[78]
Corn cob/subbit.	1.5–1.6	1.0–23.0	20/40/60/ 80	~15	N_2 100	<150	10/40	to 700	1	[66]
Yellow poplar/bit.	1.4–0.9	0.9–8.7 0.8–7.7	10/15/20/ 30	10	N_2 110	<350	5/10/15/20	to 800	1	[105]
Switchgrass, corn stover/bit.	1.6–2.9/ 1.3–5.0	0.7–11	20	4.5–5.5	N_2 80	C: <400 B: 400-500	5/10/20/40	to 800	1	[106]
Rice straw, sawdust/ bit.	2.0–11.0/ 1.6–1.0	0.78–11.43	20/40/60/ 80	nr	N_2 150	180–250	5/10/15/ 20/25/30	to 900	1	[107]

(*continued on next page*)

Table 3 (*continued*)

Biomass/coal type	Biomass(es)	Coal(s)	Blend ratios (Biomass wt %)	Capacity (mg)	Gas flow (mL/min)	Particle size (μm)	Heating rate (°C/min)	Temperature (°C)	Pressure (bar)	Ref.
	H/C molar ratio - Ash (%, db[a])									
Platanus wood/lig., bit.	1.5–0.8	0.8–24.3/ 0.5–6.0	30/50/70	10	N_2 60	<74	10/20/40	to 950	1	[108]
Giant reedgrass/lig.	1.7–16.3	1.2–21.0	10/20/30/ 40/50/60/ 70/80/90	10	N_2 60	<250	5/10/15/ 20/30	to 800	1	[109]
Chestnut sawdust/ bit., anth.	1.4–1.3	0.7–7.8/ 0.6–8.4	nr	2–5	N_2 100	<212	10/20/30	to 1000	1	[110]
Cellulose/bit.	0.7–0.1	0.7–15.4	25/50/75	~10	N_2 60		10/20/40	to 950	1	[111]
Wallnut shell/bit.	nr	nr	50	10 & 20	N_2 200	<100	50	to 900	1	[112]
Corn stalks/lig.	1.7–16.3	1.2–21.0	50	15–20	Ar 100	<1000	20	to 800	1	[80]
Leaves, softwood, hardwood/subbit	1.7–3.2/ 1.7–1.9/ 1.8–3.3	0.9–3.9	25/50/75	3–4	N_2 20	<150	20	to 800	1	[113]
Poplar/lig.	1.6–5.8	0.7–9.6	4/8/12/16/ 32	10	50	74–150	10/20/30	to 1000	1	[114]

[a] d.b. – dry basis.
[b] nr – not reported.
[c] Lig – lignite.
[d] Subbit. – subbituminous.
[e] Bit. – bituminous.
[f] Anth. – anthracite.

3.1. Yields and product distribution

In an attempt to efficiently compare conclusions, thermogravimetric studies have been critically compiled (Table 3). Further discussions will be based on studies that rigorously prepared controlled samples and performed a temperature calibration of their instrument. The dynamic mode is usually preferred to the isothermal mode as it presents the advantage of studying the entire temperature range. Unfortunately general precautions to avoid misleading measurements are often dismissed [86].

In this section various parameters of the co-pyrolysis process are fundamentally evaluated and the effect of torrefaction on these parameters is discussed. A summary of the effect of torrefaction on parameters of the co-pyrolysis process is presented in Table 5.

3.1.1. Influence of initial mass and internal heating rate: mass transfer limitations

Good practices in thermogravimetric studies require several preliminary studies that evaluate possible limitations in mass and heat transfer and guarantee that pyrolysis rates are reaction controlled. According to our knowledge, no co-pyrolysis work reports an effective and thorough study on the inherent impact of mass and heat transfer related to the initial mass. A few classic studies have reported the existence of a thermal lag (i.e. difference between reactor and sample temperature) which is a consequence of biomass pyrolysis endothermicity (discussed in Section 3.1.3) [115,116]. To overcome transport limitations, it is necessary to evaluate the influence of initial sample mass on the devolatilization behaviour. This was well illustrated by Volker and Rieckmann [117] where the influence of initial sample mass of cellulose was revealed by recording the char yield (Fig. 4). They demonstrated how mass transport significantly affects the product distribution. At a low heating rate of 3 K/min, no variation between degradation temperature range (between 593 and 595 K) and maximum decomposition rate was observed. However, the char yield increased from 2 to 18%. For higher temperature ramps, 41 and 105 K/min, significant changes in degradation temperatures and devolatilization rates were reported when increasing the initial sample mass: temperatures shifting towards higher values (from 634 to 651 K for 41 K/min) at maximum degradation rates, which are lower in consequence. This phenomenon has also been reported by other researchers for both raw and torrefied biomass pyrolysis [118]. In addition to these results, the irregularity in char yield trends at high heating rates (105 K/min) and larger samples (20–54 mg) reflects the inhomogeneity of degradation temperature within the sample due to heat transport limitations (Section 3.1.2). As a conclusion, mass transfer limitations will strongly affect resulting char yield.

For modelling purposes, mass transfer phenomena within the particle are conveniently described with a convective transport equation and gas flow with the incorporation of the Darcy's law that includes the feedstock permeability [120]. The permeation rate of gas depends on the properties of the feedstock such as permeability and porosity. This means that for feedstocks with different pore morphology, volatiles will be released at different rates during co-pyrolysis. The addition of torrefied material where the permeability of the biomass was increased during torrefaction (10^{-14} m^2 for wood and 10^{-11} m^2 for char), improves the release of volatiles by minimizing intraparticular secondary reactions [121].

The change in permeability by torrefaction depends on the temperature at which the biomass is torrefied. For example, Rousset and Girard [122] determined the effects of torrefaction at 200 °C on two mass transfer properties of Poplar wood: mass diffusivity and air permeability. They observed that torrefaction pre-treatment decreased the magnitude of mass diffusivity but no significant change in the permeability was observed which demonstrated that the thermal pre-treatment at 200 °C did not affect the pore morphology of the wood. Mafu et al. [27] also observed no significant change in CO_2 micropore surface area of woody biomass after torrefaction at 260 °C; however, when the temperature was increased to 300 °C the micropore surface area started to increase [123]. The significance of torrefaction on mass transfer during co-pyrolysis therefore strongly depends on the torrefaction temperature.

3.1.2. Influence of particle size and internal heating rate: internal and external heat transfer limitations

The presence of a temperature gradient within the particle is a direct expression of thermodynamic properties of the materials. In their review, Antal and Varhegyi [124] summarized the early efforts in rationalizing the heat transfer limitations and their impacts on kinetics. The most emblematic work remains the theory proposed by Pyle and Zaro [125]. Based on physical/structural and thermal properties of a particle, they proposed different ratios (the Biot number and Pyrolysis numbers) to assess the relative importance of internal and external heat transfers.

Experimentally, the reactor heating rate can be programmed and

Table 4
Summary of process parameters for co-pyrolysis studies using torrefied biomass and coal.

Feedstock			Torrefaction			Torrefied biomass blend ratios (wt%)	Pyrolysis					Ref.
Coal	Raw biomass	Torrefied biomass	Reactor type	Capacity (g)	Temperature (°C)		Capacity (mg)	Gas flow (mL/min)	Particle size (μm)	Heating rate (K/min)	Temperature (°C)	Pressure (bar)	
H/C molar ratio - Ash (%, db[a])													
0.7–7.5	2.1–16.0	1.3–18.0/ 0.9–24.5	Fixed bed	5	250, 300	25/50/75	8	N_2, 50	95–125	20	900	1	[131]
1.1–20.0/ 0.9–28.6/ 0.6–19.1	1.9–3.2	1.7–9.3	Tube reactor	nr[b]	250	20/50/80	nr	N_2, 20	<125	10	900	1	[135]
0.7–13.7	1.2–0.0	1.1–0.3/ 0.7–0.8	NR[b]	9.5	250, 300	25/50/75	5	N_2, 100	74–149	20	800	1	[63]

[a] d.b. – dry basis.
[b] Nr – not reported.

Table 5
Summary of the effects of torrefaction on different co-pyrolysis process parameters.

Co-pyrolysis process parameter	Effect of torrefaction
Mass transfer limitations	Less due to an increase in biomass permeability
Heat transfer limitations	Less due to an increase in biomass thermal conductivity
Enthalpy of pyrolysis	Greater due to a decrease in hemicellulose content and secondary reactions
Blend ratio	Less significant due to higher similarities with coal
Inherent organics	Twice the amount of raw biomass, but organic composition unchanged
Temperature	Higher temperature required due to the removal of light reactive volatiles
Pressure	More significant effect on product yields due to increased porosity of biomass

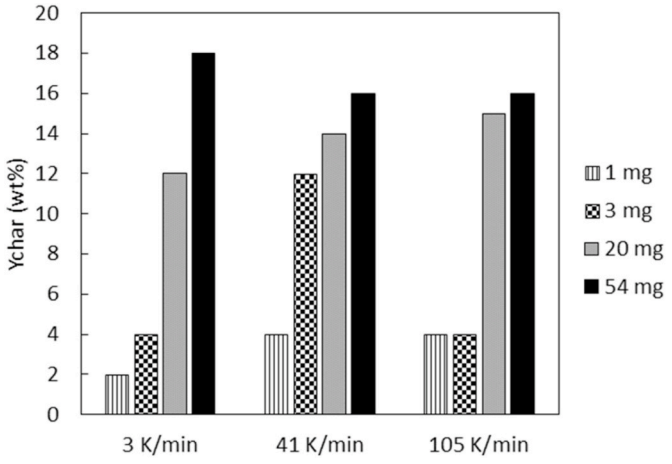

Fig. 4. Influence of the initial sample mass on char yield during the cellulose pyrolysis adapted from Volker and Rieckmann [119].

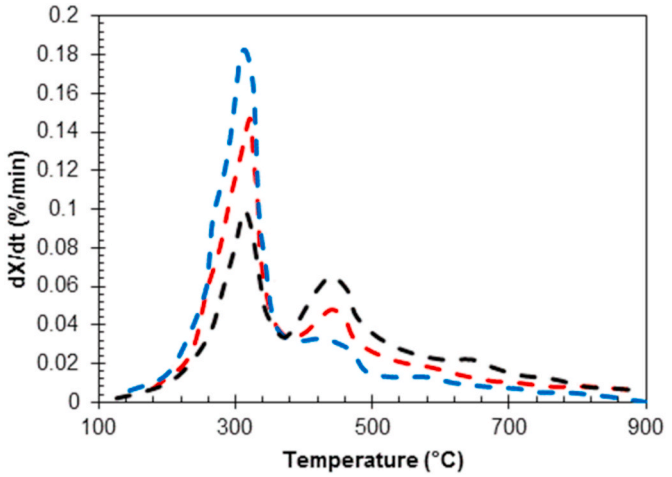

Fig. 5. DTG curves of rice straw and coal blends of (– -) 75 wt% (– -), 50 wt% and (— —) 25 wt% (Adapted from He et al. [131]).

regulates external heat transfer limitations, the extent of which depends on the type of reactor and associated heating source. Although more elaborated models are required to illustrate the influence of reactor heating rate [126], Lédé et al. [127] could estimate the extent of the thermal lag according to the reactor heating rate for different heat transfer coefficients, h in W m^{-2} K^{-1}, and initial particle sizes, L_0 in μm. The thermal lag increases with increasing heating rate and remains

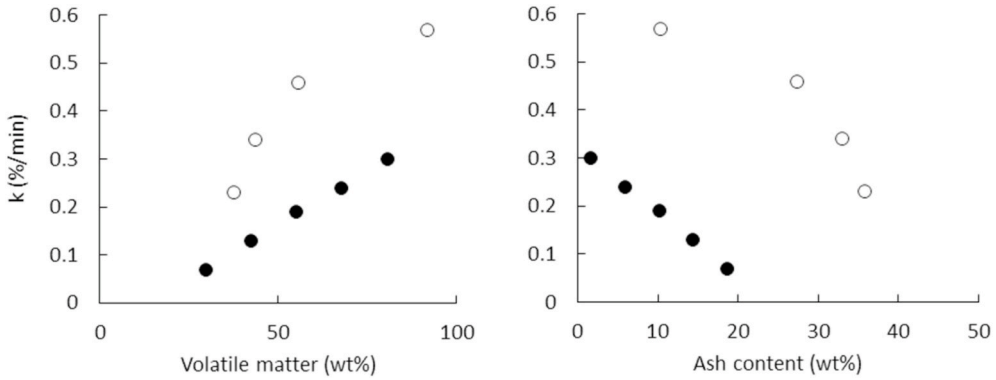

Fig. 6. Maximum pyrolysis rate of the first degradation stage (both Y-axis) versus volatile matter and ash content: (o) data obtained at 50 K/min with bagasse/coal blend from Aboyade [100] and (●) data obtained at 40 K/min with corn cob/coal blend from Wang et al. [66].

negligible at a high heating ramp for extremely low $L_0/h < 2 \times 10^{-8}$ W $m^{-1}K^{-1}$, design and operating conditions difficult to apply.

Once again, the scrutiny of existing phenomenological models is of interest to understand how changes in thermo-physical and transport properties of torrefied material may impact heat transfer. For example, Mason et al. [128] reported that torrefied wood had a significantly higher thermal conductivity (0.29 W m^{-1} K^{-1}) compared to raw biomass (0.16 W m^{-1} K^{-1}). The change in this thermal property alone is estimated to decrease the Biot number by almost a factor of 2. This means that internal temperature gradients are expected to be significantly reduced for torrefied biomass compared to raw biomass.

3.1.3. *Internal energy of pyrolysis*

The thermodynamic nature of co-pyrolysis is conventionally assessed from heat profiles that indicate the following: an early and sharp endothermic peak at temperatures below 150 °C related to surface water evaporation (dehydration) for both biomass and coal, and the highly exothermic profile of biomass compensating the endothermic character of coal conversion [93]. Chemical changes brought about by torrefaction are partly responsible for the changes observed in heat flow curves of torrefied biomass. DSC curves obtained for biomass and torrefied biomass under conditions where heat transfer limitations were minimized demonstrated that the exothermal peak observed in the range of 100–260 °C for biomass was absent for torrefied biomass and was attributed to the reduction of hemicelluloses [61]. Lignin and hemicellulose pyrolysis is exothermal but cellulose pyrolysis is endothermal [129]. The overall enthalpy of reaction of a torrefied material therefore depends strongly on the composition of biopolymers remaining in the material after torrefaction.

Furthermore, mass and heat transfer limitations may also affect the thermodynamic nature of the pyrolysis process itself. In extreme cases, extensive mass transport resistances can lead to the occurrence of highly exothermic secondary reactions; resulting in a significant decrease in the overall reaction enthalpy [119]. As discussed in Section 3.1.1 and Section 3.1.2, the torrefaction pre-treatment step significantly changes the thermo-physical and transport properties of biomass in favour of reducing mass and heat transfer limitations and secondary reactions. It would therefore be expected that the overall enthalpy of pyrolysis of torrefied biomass would be greater compared to raw biomass due to less exothermic secondary reactions.

3.1.4. *Influence of blend ratios on 'reactivity'*

Conventionally, a co-pyrolysis study reports trends illustrating the impact of the blend ratio with the intention to manipulate the stoichiometry of the pyrolysis reaction. Natural polymer mixtures are a combination of biomass with 'ideally' higher H/C ratio, O/C ratio and volatile matter content than those of coal (Table 1). The reactivity of these mixtures towards pyrolysis conditions are interpreted based on the following devolatilization patterns (Fig. 5): number of DTG peaks, shift of onset temperatures and peak temperature, maximum decomposition temperature and associated decomposition rate [130].

It can be observed on DTG curves (Fig. 5) that blending affects the shape of peaks (with or without shoulders) and their maximal degradation temperatures. If the nature of polymers and blend ratios are judiciously chosen, the maximum decomposition rate significantly increases with increasing H/C and O/C ratios and volatile matter content, which results from increasing the mass fraction of biomass [109,132]. Few studies have revealed a good relationship between the maximum decomposition rate and biomass blend fraction which is directly related to the initial volatile matter content of the blend. To depict this trend, the maximum devolatilization rate versus ash content and volatile matter of original blends (calculated as the weighted sum of the measured value of the contributing coal and biomass fractions and expressed on a dry ash free basis) have been plotted (Fig. 6).

On the same additive principle, past contributors have quantitatively assessed synergisms or/and antagonisms during co-pyrolysis and contradictory conclusions were reported mainly based on the lack of systematic evaluation approaches. In the case where synergisms/antagonisms events were depicted, the authors have systematically speculated that the higher hydrogen content in biomass plays a key role as H donor to facilitate coal degradation [70,81,93] referring to emblematic works such as Stiller's one [133]. Making use of co-liquefication agents, they illustrated how well-known hydrogen-transfer and/or termination agents for free radicals could affect the overall conversion by preventing radical recombination reactions (i.e., polymerization, cross-linking, termination). Further mechanistic aspects of co-pyrolysis are discussed in Section 3.2.

On the other hand, the influence of atomic O/C ratio is almost never invoked even though lignocellulosic biomass displays molecular ratios up to three times higher than those of coal (Table 1). The presence of higher oxygen could occasion antagonism events. Indeed, oxygen is a well-known cross-linking agent, which could counteract the effect of hydrogen [15,134].

When considering blending torrefied biomass and coal it is clear that studies are lacking (Table 4). Lu et al. [63] first reported the impact of torrefied material on the overall co-pyrolysis and concluded that whether raw or torrefied materials with low ash content were used no synergistic and/or antagonistic effects were observed based on the additive approach. In the same line, He et al. [131] reported slight deviations for char and volatile yields during the co-pyrolysis of both raw and torrefied materials (rice straw with a high ash content) and coal. However, substantial changes in degradation temperature ranges and curves shape were observed when 'severe' torrefied biomass was co-pyrolysed instead of raw material: the onset temperature of the first degradation stage shifted towards higher temperatures and degradation stages overlapped so that the DTG curves displayed one peak only. This

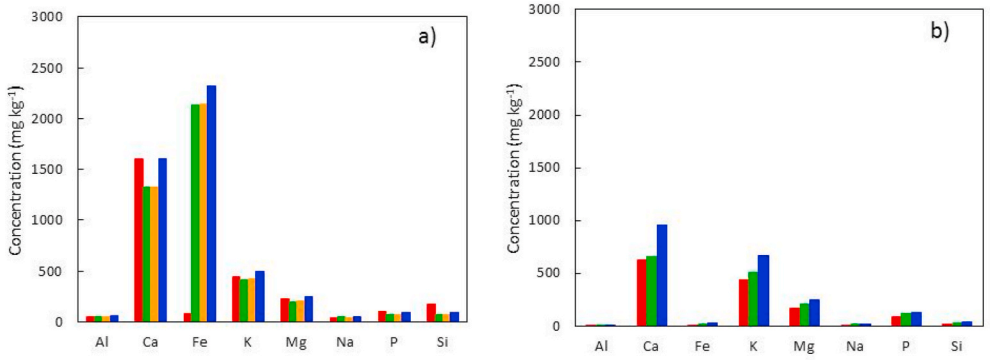

Fig. 7. Influence of torrefaction treatment on inorganic distribution within woody materials: a) Raw poplar wood (■), torrefied at 240 °C (■), at 260 °C (■) and 280 °C (■) from Kim et al. [144] and b) Raw birch wood (■), torrefied at 240 °C (■) and 280 °C (■) from Shoulaifar et al. [145].

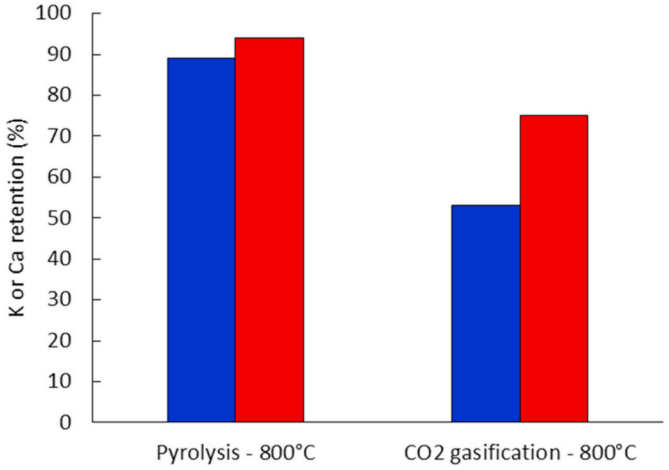

Fig. 8. Stabilization of K (■) and Ca (■) within biochar or ash after pyrolysis and CO_2 gasification (Adapted from Feng et al. [149].

last observation indicates that physical and chemical changes induced by torrefaction make the feedstock behaves more similar to coal so that the blend degrades like a single feedstock. As a result, the effect of the blend ratio becomes less significant than observed for raw biomass/coal blends.

3.1.5. Influence of inherent inorganics

The composition of biomasses and coals vary to a large extent (Table 1), particularly in the content of inorganics. Inorganics can exist naturally within the biomass under various mineral classes (silicates, oxyhydroxides, sulphates, phosphates, carbonates and others) and different states (crystalline, semi-crystalline or amorphous solids, fluid, liquid or gas) [136], but can also be added via impregnation to functionalize and/or protect the biomass and/or be added as heterogeneous catalysts (extraparticle) to influence the pyrolysis chemistry [137]. The influence of the inherent inorganics has been demonstrated several times. Listed as natural, primary/secondary catalysts [137], those elements have been shown to induce significant changes in terms of pyrolysis reactivity according to their speciation through inhibitory and/or catalytic mechanisms [138,139]. In general, the pyrolysis process concentrates the inorganic fraction in the solid carbonaceous residue [140]. A brief analysis of experimental findings indicates that the extent of alkali and alkaline earth metals influence depends on their electronic form. In the form of salt, inorganics can facilitate the depolymerisation of lignocellulose through carbon-carbon bond cleavage and by decreasing the decomposition temperature [141]. In the specific case of cellulose, these inherent inorganics were found to act on primary pyrolysis reactions resulting in significant changes of the organic products distribution [141]. It is therefore not surprising to note that a few authors working on co-pyrolysis have pointed out their role to explain some of the synergisms/antagonisms during co-pyrolysis.

Under mild conditions (torrefaction), these inherent organics are concentrated to a lesser extent than under pyrolysis conditions. As a result, the ash content of torrefied materials is generally twice that of raw biomasses [142], however the inorganic composition of raw and torrefied biomass generally remains unchanged [143] (Fig. 7a and b).

The behaviour of inorganics is rationalized according to their natural association with biomass, mineral group and classes [136]. Mineral constituents belong to different categories, for example: post-transition metals for Al, Alkali earth metals for Ca and Mg, transition metals for Fe, Alkali metals for K and Na, reactive non-metal for P and Metalloid for Si. Depending on the temperature stress level, the stability of those minerals changes. In particular, mineral phases associated with alkali and alkaline earth metals (AAEMs) are highly reactive during biomass processing and catalytic effects are often reported [146].

The inorganics are relatively well bound with solid residues and most of them remain sequestered in the carbon matrix exhibiting new catalytic functionalities. Their presence confers new functionalities that have been evidenced at enhancing feedstocks conversion during CO_2 gasification [147] and in upgrading chemical composition of pyrolysis bio-oils [148].

Textural characteristics and new surface functional groups of torrefied materials/biochars are often invoked to explain their catalytic performance; keeping in mind that one of the major issues in catalysis over biochars is related to mass transport limitations (in other words, access to the active sites) due to their microporosity. To overcome those limitations, prior activation treatments are required to investigate the intrinsic catalytic role of inorganics [149]. For this reason, the work of Feng et al. [149] is quite insightful as it reveals the mechanistic details of tar reforming at the active site scale. They overcame potential mass transfer limitations by removing primary minerals using a mild acid solution and controlled the loading of K and Ca by impregnation. To explain the higher devolatilization trait of K in comparison to Ca during CO_2 gasification (Fig. 8), the authors invoked the higher valence state of Ca facilitating its anchorage to solid. Bonds are easily broken by free radicals under an oxidant atmosphere, which is not the case in a neutral atmosphere (Fig. 8). Measured char reactivity is also greater for K than Ca, 8.87% against 6.33% respectively under CO_2 gasification. This is explained by the presence of crystal defect (C–O–K clusters) which combined with electronic properties of the biochar surface, exhibit an enhanced charge distribution on the surface, weakening chemical bonds (further details in Section 3.2.1).

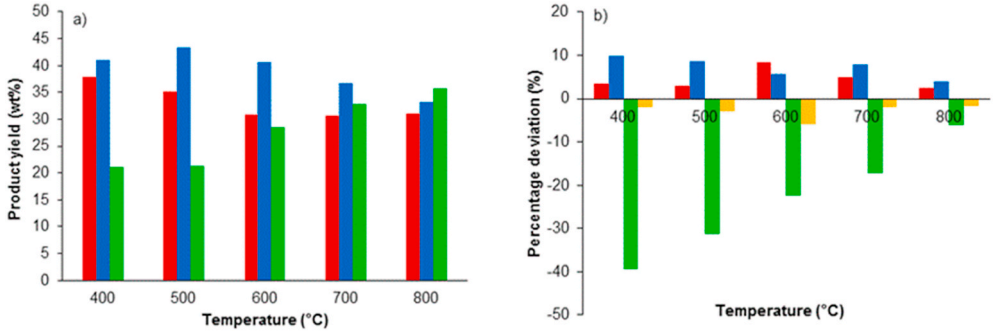

Fig. 9. Effect of temperature on a) product yield distribution from co-pyrolysis of sawdust and coal (60 wt% biomass blending ratio) in a semi-batch drop tube (■ char, ■ liquid, ■ gas), b) Deviation between experimental and calculated product yields (■ char, ■ liquid, ■ gas, ■ H_2).

With a smaller number of active sites combined with a limited access to these sites, torrefied materials should exhibit a lower catalytic activity than biochars. And if there is any catalytic effect noted, this should be mainly attributed to metallic active sites instead of acidic sites (O-containing functional groups on the surface).

3.1.6. *Influence of temperature*

The reactor temperature plays a major role in the extent of pyrolysis conversion and therefore pyrolysis product yields [150]. As the temperature increases, more volatiles are produced (gases and condensables) going through an optimum liquid yield, which consists of a compromise between the amount of volatiles released at high temperatures and the limitation of secondary cracking reactions at these conditions. The optimal temperature for liquid production differs according to different reactor configurations (Section 4.2). Usually optimal temperatures are expected to be in the order of 400–550 °C for biomass [151,152] and 500–650 °C for coal [70,153]. If temperature is increased above these optimal temperature ranges, a transition is observed in the volatile distribution towards less liquid product and more permanent gases [154].

To maximize the extent of interactions between volatiles of different feedstocks, it is recommended to produce sufficient amounts of intermediate by-products (e.g. radicals, carbocations, hydrogen donors) from coal and biomass during co-pyrolysis without producing too many non-condensable gases [70]. It would therefore be expected that the extent of synergies will be maximized at temperatures in the range of the optimum temperature for liquid production. Indeed, various authors have reported this observation [70,81,155]. The product yields obtained from the work of Park et al. [81] in a semi-batch drop tube reactor using a biomass blending ratio of 60 wt% for different temperatures is shown in Fig. 9a. The percentage deviation from calculated values is shown in Fig. 9b. It can be observed that the maximum deviation in char yields is observed at 600 °C, whereas the deviation decreases with a further increase in temperature.

The decrease in the extent of synergies with increasing temperature has also been explained by considering the increased production of hydrogen from coal at higher temperatures [13]. If the observed synergies are explained by hydrogen donors from biomass preventing the recombination reactions of coal radicals, it is suggested that when the amount of hydrogen released from coal reaches the level of that of biomass (at higher temperatures) it would result in a decrease in the extent of synergies observed. From Fig. 9b, it can be observed that the negative deviation in hydrogen yield is most significant at 600 °C when synergistic effects are maximized and becomes less significant with an increase in temperature. Another explanation is that an increase in temperature also results in an increase in gas space velocity, which leads to a shorter residence time and less interaction of volatiles with char further explaining the decrease in the extent of synergies at high temperatures [78].

For torrefied biomass, the optimum pyrolysis liquid production is significantly affected by the torrefaction processing temperature and holding time [156]. It may be expected for mixtures of coal and torrefied biomass that the optimum temperature for maximizing synergies would occur at a higher temperature than when using raw biomass. The reason being that the light and reactive volatiles produced at lower temperatures for pyrolysis of raw biomass will be absent for torrefied biomass.

3.1.7. *Influence of pressure*

Although the effect of pressure on pyrolysis product distribution has not been reported as extensively, it remains an important process parameter that primarily affects secondary reactions. Pressure is usually reported to have a negative effect on pyrolysis liquid product yields for pyrolysis of individual fuels [157,158] as well as co-pyrolysis [65,79,159].

The pressure affects the volatile residence time and vapour pressure and therefore the number of heterogeneous (char-gas) and homogeneous (gas-gas) secondary reactions [150,160]. At a high reactor pressure, a smaller pressure gradient exists between the internal and external surface of a pyrolyzing particle. Considering Darcy's law, this results in a lower velocity of the volatile products out of the particle's pores and therefore increases the char-gas contact time to favour recombination reactions. This generally results in higher char yields and lower liquid yields with increasing pressure. However, it is also possible that the volatiles remaining in the char pores will undergo thermal cracking to form gas products in which case the char yield will not be

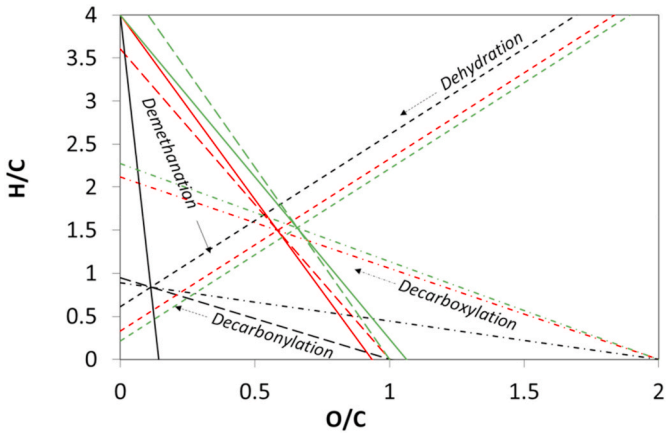

Fig. 10. Van Krevelen diagram to illustrate major devolatilization events (— dehydration, —— demethanation, -·-· decarboxylation and – – decarbonylation) during pyrolysis of (■) coal [165] (■), biomass torrefaction [166] and (■) biomass [166].

affected. Sathe and co-workers [161] reported that the extent of thermal cracking or recombination reactions occurring at different pressures in a specific reactor setup could be the controlling factors for the observed trends in char and gas yields. For example, Wafiq et al. [162] observed a decrease in char yield with increasing pressure up to 15 bar but no further changes at higher pressures. This suggests that as the external pressure is increased to 15 bar volatile trapping increases and recombination reactions dominate; therefore, higher char yields are obtained. However, with a further increase in pressure (and volatile trapping), thermal cracking reactions increase more severely and counteract the recombination reactions so that the char yield remains unchanged. Under low pressures, the residence time of highly reactive volatiles is limited resulting in a good compromise between char and liquid yields [160]. Most importantly, the pressure impacts the physico-chemical properties of products, in particular those of oil and char: the composition of oils is altered [163] and chars display substantial changes in surface areas [162].

With regards to torrefied biomass, Wafiq and co-workers [162] reported similar trends for the effect of pressure on char yields for both raw and torrefied biomass. However, pressure had a more significant negative effect on liquid yields for torrefied biomass. For raw biomass, the liquid yield decreases from 16–11 wt% d.b when pressure increased from 1 to 30 bar, whereas the liquid yield for the torrefied biomass decreases from 16–6 wt% d.b for the same pressure range. This may be due to the increased porosity of torrefied material, which weakens the internal forces by supplying a greater volume for volatiles to evolve. Consequently, more cracking reactions are expected inside the pores. The effect of pressure on co-pyrolysis of torrefied biomass and coal compared to raw biomass and coal is summarized in Table 5.

Due to increased secondary reactions at high pressure, the extent of synergies usually also increases with pressure. For example, Collot and co-workers [65] observed a deviation of 15% in liquid yields at 5 bar compared to 22% at 20 bar. Huang and co-workers [159] also reported the maximum deviation in char and liquid yields at 30 bar. The control of pressure is therefore critical to favour the extent of synergies during co-pyrolysis.

3.2. Chemistry and physics of co-pyrolysis products

3.2.1. Composition and texture of chars

Residual solids rich in carbon are important in the overall pyrolysis process as they concentrate a significant amount of energy and inorganics. The char yields resulting from co-pyrolysis of raw biomass and coal are usually lower than theoretical ones determined by the additive method [43,70]. The hydrogenation synergistic mechanism on coal pyrolysis (e.g. recombination of coal pyrolysis radicals with biomass hydrogen donors preventing polymerization reactions) is invoked to explain the residual solid decrease and the subsequent impact on the solids properties.

The formation of char can occur through various mechanisms: (1) dehydration leading to primary char and/or (2) recombination between reactive and volatiles fragments into char via cross-linking and condensation resulting in secondary char [164]. Under pyrolysis conditions, dehydration, decarbonylation, decarboxylation and demethanation reactions drive the formation of char (Fig. 10). However, under torrefaction, the dehydration remains the dominant mechanism. This prior loss of H and O during torrefaction pre-treatment with the release of water and oxygenates compounds containing carbonyl and carboxylic groups has a drastic impact on decarbonylation and decarboxylation reactions during the co-pyrolysis of coal and torrefied biomass (Fig. 10). For example, less vapour water could prevent water–gas shift reactions and limit H_2O and CO_2 gasification reactions, thus preventing the consumption of C and limiting the textural evolution of char [164]. This explanation could suggest that the conversion of the two fuels, coal and torrefied biomass is independent. It would not be surprising to observe fewer synergistic/antagonist effects during co-pyrolysis of coal and torrefied biomass in comparison to coal and raw biomass co-pyrolysis.

The decrease of both H/C and O/C molar ratios of bulk solid during biomass and coal co-pyrolysis have shown to be accompanied with a surface functionalization [123,167]. Coal, raw biomass and torrefied biomass undergo some important chemical and structural changes during pyrolysis, which have been depicted via a series of analytical approaches [168–170]. The charring process is predominantly accompanied with the aromatization of the solid matrix, which may be observed through advanced solid state C-13 NMR techniques. The inception of carbon aromatization of biomass solids during torrefaction/pyrolysis was observed at 300 °C corresponding to the start of carbohydrates conversion with the predominance of the aromatic character at 350 °C [171]. More significant changes of aromatization degree and amorphous carbon content are observed in biochar in comparison to coal char residues during co-pyrolysis. The increasing severity of torrefaction limits those morphological changes leading to a lower graphitization degree and an increased amorphous carbon content of biochar during co-pyrolysis of torrefied biomass and coal. On the other hand, the aromatization of the coal char as well as the amorphous carbon content remained quasi unchanged whatever the torrefaction temperature [131].

Another important factor which affects the co-pyrolysis char structure is the biochemical composition of the biomass. During torrefaction this composition alters mainly due to the degradation of hemicelluloses [172]. The effects of the addition of these biopolymers on the structural transformation in aromatic ring systems of co-pyrolysis char have been reported: the addition of cellulose resulted in a decrease in small (3–5 ring) aromatic structures in co-pyrolysis char, whereas the addition of lignin promoted them and lead to a lower degree of ordering in the char [173]. He and co-workers [131] reported that the char surface of torrefied biomass and coal co-pyrolysis char was more disordered than when raw biomass was used which may be linked to the relatively higher amount of lignin in torrefied biomass.

Few authors have reported the critical role of inorganics in the char functionalization but also in its structural reorganization. In general, the alkali and alkaline earth metallic (AAEM) species have been reported to break weak bonds to the benefit of stronger bonds, increasing the surface proportion of condensed aromatic rings [174]. In the case of torrefied biomass (with a higher amount of inorganics) an increase in the extent of these reactions occurs which may explain the increase in condensed aromatic carbons reported for the pyrolysis char [175]. This trend highly depends on the nature of AAEM present within feedstocks. Indeed, opposite tendencies were observed in the presence of high Ca and K levels that promote demethoxylation reactions [95]; thus, preventing the methoxyphenols known as promotors of aromatic structures to play their role of char aromatization [176].

Shape transition of torrefied materials/biochar has been reported a few times using SEM analysis. The shape of particle evolves with the severity of pyrolysis and depends on temperature [104,177]. The observation of needle-like particle transformation into lamellate particle has been quantitatively confirmed by measurements of carbon lattice, which stretched into sheets as temperature increased [123]. These structures are both driven by the original lignocellulosic composition of feedstocks [123,171,173].

Characterizing the whole structure of char is challenging as their

Table 6
Summary of the effect of torrefaction on co-pyrolysis char structural properties.

Co-pyrolysis char property	Effect of torrefaction
Graphitization degree	Low
Microporosity	High
Degree of aromaticity	High
Amorphous carbon	High
Particle shape	Mainly lamellate

Table 7
Properties of oils derived from pyrolysis and co-pyrolysis of biomass, torrefied biomass and coal.

Pyrolysis oil property	Raw biomass	Torrefied biomass	Coal	Biomass and coal
Yield (wt%)	65-75 [7]	34-55 [20]	6-25 [9]	7-41 [72,85]
Chemical components	Acids, alcohols, aldehydes, ketones, phenols, guaiacols, syringols, anhydrosugars, furans, alkenes, PAHs, nitrogen compounds, and miscellaneous oxygenates		Light-benzene, toluene, xylenes, styrene, phenols, pyridine, anilines and quinolones	Combination of raw/torrefied biomass and coal derived components
Water content (wt% of liquids)	15-30 [184]	7-26 [185,186]	2-5 [9]	7-20 [77]
Elemental Analysis (wt% d.a.f.)	[187]	[186,188]	[9]	[85]
Carbon	42–47	45–66	80–85	73–75
Hydrogen	6–8	5–8	2–8	11–12
Oxygen	46–51	23–46	6–8	12–15
Nitrogen	< 0.1	<0.8	<1.1	1.3–1.6
Sulphur	< 0.02	nr[a]	<0.4	Nr
HHV (MJ/kg)	17-20 [186, 187]	17-27 [20,186]	46 [189]	38-40 [85]

[a] Nr – not reported.

analysis is limited by their amorphous and microporous character. BET porosity description remains poor as gas diffusion is often hampered by the size of pores. When CO_2 adsorption is used, specific surface areas measured can reach until 170 m^2/g for torrefied biomass at 290 °C [178, 179]. Variations in pore size distribution during the torrefaction process was also observed: initial macropores are transformed into mesopores for mild temperature (260 °C), pores that become essentially macro- and micropores at higher temperature, 290 °C. Combined with a loss of hydroxyl groups, the extent of microporosity is suspected to contribute to the hydrophobicity of torrefied material [178]. Microporous structure of torrefied materials is also invoked to limit reactants diffusion within the particle [149], which has incited the scientific community to investigate the surface functionalization of biochar on which active sites such as oxygen-containing compounds and metallic oxides are grafted. As result, torrefied material could play an important catalytic role during co-pyrolysis. A summary of the effects of torrefaction on co-pyrolysis char properties is provided in Table 6.

3.2.2. *Nature of volatiles and condensates*

Hot volatiles are released during pyrolysis of natural polymers and the extent of the production is subject to reactor conditions (Section 4.2). These volatiles include condensable liquids (oils) and non-condensable gases [180]. The yield and composition of oils derived from individual pyrolysis of raw/torrefied biomass and coal as well as from co-pyrolysis of raw biomass and coal are reported in Table 7. To the knowledge of the authors, no studies are yet available on the characteristics of oil derived from co-pyrolysis of torrefied biomass and coal. However, reviewing the effect of torrefaction on individual pyrolysis of biomass provides important clues as to the oil yield and composition that may be expected for co-pyrolysis since torrefaction will only affect the chemical compounds derived from the biomass fraction of the blended feedstock.

The oil from raw biomass pyrolysis has a complex chemical composition: it contains a wide range of reactive oxygenated species and a substantial portion of water (Table 7). The significant elemental oxygen proportion within bio-oil, larger than those measured in coal-derived oils, leads to premature aging, chemical instability and a lower calorific value [181]. The pre-treatment of biomass through torrefaction improves many of the characteristics of the oil (Table 7). The water content and oxygen content of bio-oil derived from torrefied material were reduced and the carbon content was increased [182]. The oil also contained significantly higher amounts of levoglucosan and phenolic compounds, and lower acid yields [183]. These changes were due to the removal of water during torrefaction, the decomposition of hemicelluloses and the increase in the relative amount of lignin in the torrefied biomass [182].

It may therefore be expected that co-pyrolysis oil derived from torrefied biomass and coal will also have lower oxygen and water content and higher amounts of phenols.

3.3. *Progress on co-pyrolysis kinetics*

Biomass and coal pyrolysis kinetics have a long history but remain a complex field [64]. At the molecular scale, there has been considerable attention towards the development of mechanistic models described as a series of first-order unimolecular reactions. The most emblematic works in coal and biomass chemical kinetics often rely on free-radical patterns without any descriptions of phenomenological events. On the other hand, kinetic approaches at the reactor level require mathematical representations of mass and heat transfer phenomena; constraining the scientific community to adopt lumping or apparent kinetic methods. These approaches result in the loss of information on certain species and reactions, but also in the physical meaning of the reaction rate constant. To overcome those disadvantages, hybrid models coupling both fluid and chemical mechanisms were developed [190,191]; however, these models often use ideal conditions and do not account properly for countless factors in the industrial reactor. Furthermore, the accurate measurement of various input parameters presents tremendous challenges.

To some extent, the exact reaction mechanism of individual pyrolysis of biomass and coal remains a mystery and the blending of these fuels during co-pyrolysis complicates it even further. The various kinetic approaches for co-pyrolysis are shown in Table 8 and it is clear that empirical/semi empirical approaches remain popular. To obtain experimental data, non-isothermal techniques are generally used due to their ability to assess a range of temperatures. Considering previous recommendations, only the collection of data under multiple heating rates that limits the dependence on the selected kinetic model will be discussed [192].

Empirical models such as Monte Carlo and Artificial Neural Network are useful for predicting complex input/output relationships in a co-pyrolysis process but a major disadvantage of these approaches is that their parameters are only applicable to the process and fuels for which they were developed [193]. Another approach involves models originally developed for coal devolatilization such as the chemical percolation devolatilization (CPD) model which is based on chemical structural parameters and uses general kinetic parameters [194]. The main limitation of these models is the large structural differences between

Table 8
Summary of kinetic approaches for co-pyrolysis of biomass and coal.

Description	Feedstocks	Target	Ref.
Empirical/Mechanistic			
Monte Carlo simulation (Parallel algorithms for unimolecular or global reactions (Statistical approach, deterministic and stochastic models)	Pentadecylbenzene and tetradecylcyclohexane;	Molecular weight, Yield	[203]
Semi-empirical (Hybrid)			
Isothermal and dynamic thermogravimetry (Arrhenius equation, 1st order model) + DAEM model + 'Lumped parameter' model	Coal, biogran, pine	Eα, A, Yield	[88]
1 Thermogravimetry (Arrhenius equation, First order model) + Distributed activation energy model (Gaussian distribution)	Energy grass and lignite; fat coal and poplar; bagasse and sludge	Eα, A, Yield	1-[109]
2 Dynamic thermogravimetry (Miura integral method) + DAEM			2-[114]
3 Dynamic thermogravimetry (Flynn-Wall Ozawa and Kissinger-Akhira-Sunose methods) + General DAEM			3-[204]
4 Dynamic thermogravimetry (Miura integral method) + DAEM			4-[200]
1 Dynamic thermogravimetry (Kissinger method)	Wood/nut shells and coal; Wood and coal	Eα, A, Yield	1- [59]
2 Dynamic thermogravimetry (Integral Flynn–Wall–Ozawa method)			2-[102]
3 Dynamic thermogravimetry (Integral method of Coats and Redfern, 5 models based on reaction mechanism function)			3-[103]
4 Dynamic thermogravimetry (Arrhenius equation, nth order model)			4- [91]
5 Dynamic thermogravimetry (Integral method of Coats and Redfern, 1st and nth order models based on reaction mechanism function)			5- [63]
Thermogravimetry (Coats-Redfern method, 17 models based on reaction mechanism function) + Artificial neural network (Back-propagation algorithm)	Rice husk and wastewater sludge	Eα, A, ΔH, ΔG, ΔS, Yield	[193]
Isothermal, Bio-Chemical Percolation Devolatilization (CPD) coupled with particle energy equation (Percolation lattice statistics)	Brown coal, bituminous coal, wheat husk and corn stalk	Volatile and char yields	[194]

biomass and coal which need to be accounted for [172].

The isoconversional methods, also called 'model-free', have received an increased interest as they do not need the knowledge of the reaction mechanism and the choice of a specific model. They are considered as a preliminary assessment of the global kinetic behaviour by providing a set of apparent kinetics parameters. The results of different co-pyrolysis studies using this approach are shown in Table 9. Only activation energies (Eα) are reported as the procedure to evaluate the frequency factor, A, remains vigorously debated. It has been found that the activation energy ranges related to the conversion of coal, 200–271 kJ/mol [59,111], are systematically higher compared to those of biomass pyrolysis, 117–183 kJ/mol, [102,132]. The effect of blending, by increasing the biomass fraction of the mixture, was also clearly evidenced: the apparent activation energy decreased significantly. Some studies reported a regular decreasing trend [59,132], while others found an optimum mass ratio of 50% where the lowest Eα is reached [104,108,111]. The variability of Eα during the whole process confirms the heterogeneous nature of the biomass and coal co-pyrolysis and suggests that a multistep model should be considered.

Among the myriad of available models, single reaction global models used in solid state reactions such as the 1st order an nth order-based models have been applied to describe concurrent and consecutive independent parallel routes (Table S4). Although these kinetic studies suggested a more intricate description of co-pyrolysis, the number of parallel reactions materialized by pseudo-components and their independence are assumed. In some cases, the selection of pseudo-components is not arbitrary. For example, a 3-pseudocomponent model is often chosen to describe biomass pyrolysis and simulated peaks attributed to the decomposition of hemicelluloses, cellulose and lignin [195]. Similar to biomass, the thermal behaviour of coal is satisfactorily described with a 3-pseudocompoment model from a product perspective (i.e. tar, gas, char) [134], but not systematically related to the maceral composition of coal (i.e., vitrinite, liptinite, inertinite) [196]. For these models, it is clear that there are many limitations of a simply curve fitting exercise, for which the extrapolation may be meaningless if physics and chemistry are not adequately described. To be consistent with the nature of biomass and coal and their devolatilization behaviour, the normalized dependent contributions of the lignocellulosic composition to the total volatile matter should be first established and the pyrolysis rate of the blend should be described as the weighed sum of each individual fuel pyrolysis rate to be representative of the mix ratio (referred to as the additive method). In general, researchers agree that the additive method is valid for modelling co-pyrolysis processes since isoconversional models demonstrate negligible deviations in Eα values between single fuels and blends. An example is shown in Fig. 11.

Another popular kinetic model, the distributed activation energy model (DAEM) is widely applied for complex pyrolysis systems and reviews on this model are available [197]. DAEM is a multiple reaction model that assumes many independent reactions taking place with each rate equation describing the total amount of volatiles released, or the amount of an individual volatile constituent. The integration of a continuous function, f(E), is used to describe the activation energy for each reaction. The average activation energy (E_0), standard deviation and in particular the shape both describe the density function, f(E).

The DAEM has been successfully used for coal and biomass pyrolysis separately [198,199] and often combined with isoconversional models in the case of co-pyrolysis studies. The performance of prediction for DAEM is improved when input variables (i.e., kinetic parameters) are first processed using free-model methods [86]. The determination of the continuous function, f(E), can be achieved through distribution-free [114,200] or distribution-fitting methods [109]. For distribution-free methods, the activation energy (E) is first estimated using the isoconversional method and then the conversion vs E relationship is differentiated by E to obtain f(E). The most popular shape for the distribution curve used is Gaussian; but others distributions (e.g., Logistic, Weibull) are proposed to account for the structural asymmetry within biomass materials [197]. A summary of co-pyrolysis studies using DAEM is shown in Table 10.

Although isoconversional approaches are useful, the selection of a model is inevitable. For co-pyrolysis, the individual fuels are usually first modelled separately and then the additive approach is used to describe the behaviour of the blends. Besides co-pyrolysis, the additive approach is common in biomass pyrolysis models where the fuel is considered a combination of cellulose, hemicellulose and lignin [201]. This approach may also be applied for torrefied biomass by adjusting the models for raw biomass due to the degradation of hemicellulose during torrefaction (Section 2.2). Researchers observed that torrefaction did not affect the

Table 9
Summary of co-pyrolysis kinetic studies using model-free models and their reported kinetic parameters.

Biomass/coal type	Blend ratios (Biomass wt%)	HR (°C/min)	Temperature range (°C)	Numerical method	Conversion (%)	Eα (kJ/mol)		Ref.
						Biomass	Coal	
Cypress wood chips/ bit.[d]	80/85/90/95	5/10/15/20	25–1000	Differential, Kissinger's method	Conversion at peak T[a]	169	200	[59]
Pine wood chips/bit.	50/100	10/20/30/40	Ambient to 1000	Integral, FWO[b]	Biomass: 20–80, Coal: 10-30	Average: 117	Average: 106	[102]
Edible fungi residue/ bit.	25/50/75	10/20/40	37 to 927	Integral, KAS[c] Integral, FWO	20–80 20–80	63–206 74–250	169–386 176–378	[104]
Plantus wood/bit.	30/50/70	10/20/40	Ambient to 950	Integral, KAS	20–80	122–208	52–214	[108]
Cellulose/bit.	25/50/75	10/20/40	Ambient to 950	Integral, FWO	20–80	121–143	169–386	[111]
BG, CC, CS/bit.	10/20/30/40/50	5/10/20/30/40/50	110 to 900	Differential, Friedman	10–80	BG[g]:165-180 CC[h]:162-190 CS[i]:160-175	Average: 246	[132]
Yellow poplar/ WC[e] bit. HC[f] bit.	10/15/20/30	5/10/15/20	500–800	Differential, Friedman	20–80	162–337	WC: 252-579 HC:164-272	[105]
Oil palm EFB[j]/subbit.[k]	50/50	10/20/40/60	Ambient to 900	Kissinger's method	Conversion at peak T	210	273	[96]

[a] T – temperature.
[b] FWO – Flynn–Wall–Ozawa
[c] KAS – Kissinger–Akahira–Sunose.
[d] Bit. – bituminous coal.
[e] WC – weak coking coal.
[f] HC – hard coking coal.
[g] BG – bagasse.
[h] CC – corncob.
[i] CS – corn stover.
[j] EFB – empty fruit bunches.
[k] Subbit – sub-bituminous coal.

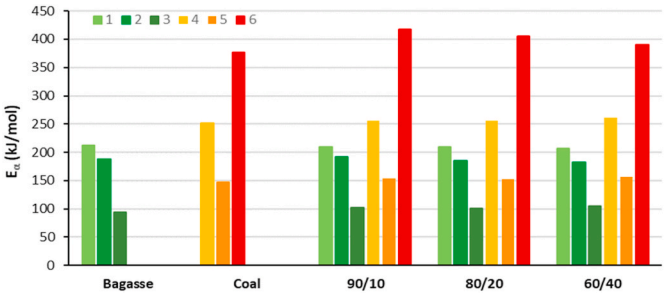

Fig. 11. Apparent activation energy for single fuels and blends (Bagasse/coal) from 6 pseudocomponents, nth model fitting based on multiple heating rate approach (adapted from Aboyade et al. [100]).

intrinsic pyrolysis kinetics of the three biopolymers but only their contribution factors [202]. Therefore, the estimation of intrinsic kinetic parameters for co-pyrolysis of torrefied biomass and coal should be possible if intrinsic parameters are available for individual pyrolysis of raw biomass and coal.

While researchers have made progress on co-pyrolysis kinetic studies, it is clear that more comprehensive kinetic studies are required in this field especially with regards to torrefied biomass and coal where only model-fitting studies are available (Table S5). It has been suggested that the best approach for kinetic modelling of a complex heterogeneous pyrolysis system is through statistical methods, which empirically correlate kinetic data from experiments [124]. However, the major drawback is that the kinetic parameters are not intrinsic and based on experimental work with specific feedstocks. The co-processing of torrefied biomass and coal results in a highly heterogeneous feedstock and the optimization of this industrial process would most likely be very challenging without the use of generalized correlations to describe reaction kinetics of various feedstocks. This emphasizes the need for developing robust kinetic models which may be applied in different pyrolysis reactors.

4. Engineering applications

After reviewing the fundamentals and kinetics of co-pyrolysis, the application of this process is now discussed. Co-pyrolysis has different applications such as the production of bioenergy or chemical products (biorefinery) and the successful design and integration of these processes is vital for its commercialization. Co-pyrolysis is a fractionation technology and is coupled to a series of engineered sections: the feeding system, heated reactor, gas/liquid/solid separation and downstream upgrading technologies. This section includes discussions on feedstock pre-treatment and reactor technologies. Downstream upgrading technologies have been the topics of other reviews [21,187,205,206].

4.1. *Pre-treatment technologies*

Pre-treatment methods have been extensively reviewed [207–211]. In this review, the focus is on techniques developed to ease the co-utilization of biomass in coal-based thermochemical conversion processes. Advantages and challenges of the techniques are summarized in Table 11.

For lignocellulosic biomass, the heterogeneity, low energy density, high moisture content and fibrous nature are major problems in the effective transport, handling and storage of the material [212]. Biofuel briquettes and pellets are a popular pre-treatment solution and their production has grown rapidly [213–217].

A challenge faced when utilizing biomass in thermochemical conversion processes is the grindability of biomass [218–220]. To improve its fuel properties, torrefaction has received considerable attention and several reviews on torrefaction are available [24,221,222]. The

Table 10
Summary of co-pyrolysis studies using DAEM and their reported average activation energies.

Model	HR (°C/min)	Numerical method	Feedstock	F(E) shape	Average E_0 (kJ/mol)	Ref.
DAEM	5/10/15/20/30	Integral, Miura-Maki method	Biomass (reedgrass)	Gaussian	134	[109]
			Coal (lignite)		221	
			Biomass blend 20/80		210	
			Biomass blend 80/20		165	
DAEM	10/20/30	Integral, Miura method	Biomass (poplar)	Gaussian	106	[114]
			Coal (fat coal)		163	
			Biomass blend 4/96		150	
			Biomass blend 8/92		118	
			Biomass blend 12/88		114	
			Biomass blend 16/84		95	
			Biomass blend 32/68		91	
DAEM	10/20/30/40/60	Integral, Miura method	Biomass (corn stalks)	Gaussian	89	[200]
			Coal (bituminous)		168	
			Biomass blend 25/75		130	
			Biomass blend 50/50		124	
			Biomass blend 75/25		88	

Table 11
Advantages and disadvantages of different physico-chemical and thermal pre-treatments methods.

Pre-treatment method	Advantages	Challenges
Pelletization/ briquetting	• Improved biomass energy density • Easy transport and handling • Reduced risk of spontaneous combustion during storage • Coal infrastructure may be used for storage, milling and feeding	• Easily absorbs moisture and swells • Sensitive to mechanical damaging during transport • Susceptible to biological degradation and fungal development during storage • Difficult to optimize process
Torrefaction	• Improved hydrophobic nature of biomass • Reduced O/C and H/C ratios • Improved higher heating value • Improved grindability • Reduced risk of biological degradation and fungal development during storage • Increased uniformity of material • Coal infrastructure may be used for storage, milling and feeding • Material may be co-utilized with coal using existing coal-based infrastructure for thermochemical conversion processes • Reduced volatile matter content	• Additional unit required in thermochemical conversion chain • Further densification of torrefied material required

torrefaction process alters the chemical and physical properties of biomass to become more similar to coal, which ensures that the biomass/coal blend can be directly introduced into the existing coal milling and feeding systems [222]. Phanphanich and Mani [212] showed that torrefaction of pine chips at 300 °C allowed the production of a much finer powder (mean particle size 130 μm compared to 710 μm for raw material) with lower energy consumption needed for milling (23.9 kWh/t versus 237.7 kWh/t) [223]. A comparison of raw, torrefied biomass and coal fuel properties is shown in Table 12.

Important parameters to consider during co-pyrolysis include the variations in particle size distribution, sphericity and particle surface area of biomass and coal (Table 13). These variations between the two feedstocks can be reduced by torrefaction. When torrefied material is milled it produces a uniform particle size distribution with more spherical particles, similar to coal. This results in a feedstock with more homogeneous properties during co-pyrolysis of torrefied biomass and

Table 13
Summary of chemical and physical properties of raw/torrefied biomass and coal [27,226,227].

Property	Raw wood	Torrefied wood	Bituminous coal
Biochemical			
Chemical constituents (wt %)			
Hemicellulose	11–13	2–3	
Cellulose	47–57	36–47	
Lignin	16–45	16–45	
Structural			
Typical particle diameter (mm)	3–50	3–50	5–40
Particle size distribution range	Wide	Narrow	Narrow
Sphericity	0.48	0.62	0.79
Micropore specific surface area (m^2/g)	84–91	84–86	150–200

Table 12
Comparison of fuel properties of raw wood, torrefied wood, raw pellets, torrefied pellets and bituminous coal (adapted from Refs. [222,224,225]).

Property	Raw wood chips	Torrefied wood	Raw wood pellets	Torrefied wood pellets	Bituminous coal
Moisture content (wt%)	30–60	1–5	7–10	1–5	5–10
Bulk density (kg/m^3)	250–400	180–300	550–700	750–850	800–1000
Energy density (MJ/m^3)	2500–3200	4600	10700	15000–17800	20000–25000
Lower calorific value (MJ/kg)	6–13	19–23	15–16	19–24	23–28
Grindability (kWh/t)	230–240	23–78	230–240	23–78	12
Water-affinity	Hydrophilic	Hydrophobic	Hydrophilic	Hydrophobic	Hydrophobic
Biological degradation	Yes	No	Yes	No	No

Table 14
Summary of main pyrolysis reactor technologies.

Reactor type	Typical scale of pyrolysis	Typical feeding system	Typical operating conditions	Target product	Product recovery	Main advantage	Main challenge	Suitability for co-pyrolysis
Fluidized bed	Commercial	Screw feeder	T[a]:400–550 °C P[b]: 1–3 atm Rt[c]: 0.3–40s	Oil	Cyclone, condenser train, electronic precipitator	High heat and mass transfer rates	Technical issues related to gas as mixing/heat interchange agent	Unsuitable, total segregation of fuel particles likely to minimize synergy
Rotating cone	Commercial	Conveyer belt feeder	T: 300–700 °C P: 1 atm Rt: <1s	Oil	Cyclone, 1-stage quenching with recycled oil	High heat transfer rates, no inert gas required	Technical issues with re-heating of sand	Suitable, close contact between particles
Ablative	Pilot plant	Screw feeder	T: 300–600 °C P: 1 atm Rt: <1s	Oil	Cyclone, 2-stage direct liquid quenching with recycled oil	Able to operate with large fuel particles (5–20 mm)	Complexity with scale-up	Unsuitable, technical issues with heterogeneous feedstock mixtures
Vortex	Laboratory	Screw feeder	T: 500–625 °C P: 1 atm Rt: <1s	Oil	Cyclone, 1-stage condenser	High heat and mass transfer rates	Complexity with scale-up	Unsuitable, segregation of fuel particles likely to minimize synergy
Entrained	Pilot plant	Screw feeder	T: 400–800 °C P: 1 atm Rt: <1s	Oil	Cyclone, 1-stage direct liquid quenching with recycled oil	No extra hot solid material needed for heat transfer	Insufficient heat transfer for short residence times	Unsuitable, total segregation of fuel particles likely to minimize synergy
Fixed bed	Laboratory	Batch loading	T:400–700 °C P: 1–30 bar Rt: 3–10s	Char	Condenser systems	Intimate contact between fuel particles	High extent of secondary reactions due to long residence times	Suitable, close contact between particles

[a] T: Temperature.
[b] P: Pressure.
[c] Rt: Vapour residence time.

Table 15
Advantages and challenges of different heat transfer modes for co-pyrolysis [5,229,264].

Heat transfer mode	Advantages	Challenges
Conduction	• High heat transfer rates between heating agent and fuel particles (>500 W/m^2 K) • Heat may be sufficiently transferred to large fuel particles • Rate of heat transfer increases with conversion due to higher thermal conductivity of char	• Direct contact required between heating agent and fuel particles can lead to solid attrition
Convection	• Reduction of solid attrition that occurs from solid-solid collisions • No additional inert solid material required	• Long gas residence times required for sufficient heat transfer • Small fuel particles required for gas/solid heat transfer
Radiation	• Fastest mode of heat transfer • Radiative heat not absorbed by gas which avoids secondary reactions	• Requires wall heating in pyrolysis reactor design • Requires concentration of radiation to produce sufficient heat transfer

coal. Torrefied biomass has a low bulk density (around 180–300 kg/m^3); however, this problem may be overcome by combining pelletization and torrefaction [224].

Economic analyses report that even though torrefaction represents an additional unit in the thermochemical conversion chain, the overall cost for torrefied biomass pellets is lower compared to regular pellets due to savings on transport, handling and storage [221,222]. In a comparative cradle-to-gate life cycle assessment of torrefied wood pellet production Adams and co-workers [225] showed that torrefied pellets offers advantages over raw pellets, but in order for the torrefaction process to be carried out at a commercial scale, end-user confidence needs to grow. As seen in Table 12, the properties of torrefied pellets are the most comparable to coal suggesting that it will be the easiest feedstock for introduction into coal-based thermochemical processes.

4.2. Types of co-pyrolysis technologies

Pyrolysis is a complex process involving both simultaneous and consecutive reactions [228]. The chemical process begins with primary thermal decomposition steps (Section 2.2) followed by secondary reactions [229]. Product yields and quality are significantly affected by process parameters including: temperature, pressure, heating rate, gas and solid residence time and particle size [230]. Pyrolysis processes therefore require elaborate control strategies to maximize the yields of targeted products [150]. Several types of pyrolysis technologies have been developed including fixed bed [231–233], rotatory kiln [234–236], auger screw [237–239], bubbling fluidized bed [240–242], circulating fluidized bed [243–247], entrained flow [248–250], rotating cone [251–253] and ablative [254–256]. The main pyrolysis technologies are summarized in Table 14 with regards to the current scale of pyrolysis, operating conditions and target products. Furthermore, the main advantage and challenges of the different technologies are reported and their suitability for co-pyrolysis is evaluated.

4.2.1. Reactor feeding systems

Typical reactor feeding systems for different technologies may also be observed in Table 14. Detailed reviews on the advantages and challenges of these systems are available [257] In general, reactors which utilize gas as mixing/heating agent use screw feeders whereas the commercial rotating cone reactor uses a conveyer belt. Kenney and co-workers [258] demonstrated how the design of these systems for heterogeneous material requires an important trade-off between expensive robust designs and improved pre-processing operations to constrain feedstock properties to the design specifications. Pre-treatment technologies (Section 4.1) therefore play a significant role in the success of a reactor feeding system.

Table 16
Summary of different co-pyrolysis technologies according to their operating conditions, product yields, heat fluxes and contribution of heat transfer modes (calculations provided in Supplementary Data Section S1).

Reactor type	Pyrolysis type	Particle size (mm)	Gas velocity (m/s)	Heat interchange	Product yield (%)	Mode of heat transfer	Estimated contribution of heat transfer mode (%)			Ref
							400°C	**500°C**	**600°C**	
Fluidized bed	Fast	<3	2	Heating by gas and sand	L[a]: 40-75					[240,243,271]
					S[b]: 10-22	Conduction	78	77	75	
					G[c]: 8-34	Convection	17	17	17	
						Radiation	5	6	8	
Rotating cone	Fast	<10	0	Heating by sand	L: 50-60	Conduction	94	92	90	[7,264]
					S: 10-15	Convection	0	0	0	
					G: 20-25	Radiation	6	8	10	
Ablative	Flash	5–20	0	Wall heating	L: 50-80	Conduction	78	72	62	[7,254–256]
					S: 15-20	Convection	0	0	0	
					G: 10-15	Radiation	22	28	38	
Entrained	Flash	<0.2	10	Heating by gas	L: 10-40	Conduction	0	0	0	[248,249,267,
					S: 8-30	Convection	99	99	99	272]
					G: 16-44	Radiation	1	1	1	
Fixed bed	Slow	3–60	0.2	Heating by wall and gas	L: 18-35	Conduction	0	0	0	[33,231–233]
					S: 25-43	Convection	84	79	72	
					G:11-38	Radiation	16	21	28	

[a] L: Liquid product.
[b] S: Solid product.
[c] G: Gas product.

4.2.2. *Reactor heating types*

Effective heat transfer in a pyrolysis reactor is paramount and mainly occurs through conduction and convection although radiation can also contribute [5]. The advantages/challenges of these different heat transfer modes for co-pyrolysis are summarized in Table 15. Bridgwater and co-workers [5] first introduced a list of pyrolysis technologies according to the type of heat transfer mode; however, the contribution of these modes for different technologies was only speculated [5,259] without reporting any calculations. In this review, basic heat transfer equations for conduction, convection and radiation were used to estimate the contribution of heat transfer types for different reactors over a range of temperatures (400–600 °C) at which most of these reactors operate. For these calculations, the different reactors were assumed to have similar dimensions, while typical particle size and gas velocity values were used. Heat transfer by conduction was assumed to occur via reactor plates (ablative) or sand (fluidized bed/rotating cone) and determined through knowledge of the thermal conductivity of these materials. Convective heat transfer occurred via inert gas and could be determined from the Nusselt number obtained through the Whitaker correlation [260]. Heat by radiation was determined through knowledge of emissivity of sand and reactor walls/plates. The results of these calculations as well as typical product yields for different reactors are shown in Table 16. Details of the calculations are provided in the Supplementary Data Section S1.

It can be observed from Table 16 that the contribution of heat transfer type depends on the reactor configuration. In ablative reactors heat is transferred directly from the hot plate surface to the biomass particles contacting the wall through conduction [261]. Aston University developed an ablative reactor and obtained up to 80% bio-oil yield [262], but the commercial implementation of this process is challenging due to the complexity in scale-up [259]. Fluidized bed reactors use recirculating hot sand to transport heat to biomass particles through conduction [259]. Although this technology has been commercialized by Dynamotive, major technical obstacles lead to the cease of operation [263]. A problem related to this design is that the gas used for mixing comes from the un-condensable gases produced during pyrolysis which constantly requires cleaning and recompressing, resulting large peripheral equipment [264]. Furthermore, the gas is a poor mixing agent and merely goes the way of lowest pressure difference, therefore playing no role in the prevention of clustering/blockages. The technology is also not well-suited for co-pyrolysis where synergetic effects are desirable in terms of oil yield. To achieve synergy, the extent of contact between the fuel particles is an important factor [265] and the near total segregation of the sample particles is likely to minimize the interaction between biomass H-donors and coal radicals [16].

Most co-pyrolysis studies have used lab scale fixed bed reactors [43,65,75,79,81]. Some authors suggest that the large amount of sample and intimate contact between the particles and volatiles in this reactor result in synergy. Many secondary reactions occur in a fixed bed due to the long residence time of volatiles; therefore, it is difficult to determine whether the occurrence of synergy is due to primary pyrolysis or secondary reactions of volatiles [19].

Entrained flow pyrolysis reactors are operated at high gas flow rates and heat transfer occurs almost entirely through convection [266]. The main challenge is obtaining a sufficiently high heat transfer in the short gas residence time [267]. Georgia Tech Research Institute [259] observed that longer gas/vapour residence times were needed to ensure sufficient heat transfer but this results in more cracking reactions, therefore lower liquid yields. The short residence time of volatiles in the entrained flow reactor makes it less suited to achieve synergy during co-pyrolysis [268,269].

The University of Twente together with the BTG group developed a rotating cone reactor [270]. Originally the design relied solely on an ablative principle but later research stated that the most effective way to transfer heat was to mix the biomass with pre-heated inert sand particles. The large surface area provided by the sand ensures sufficient heat transfer to the biomass by conduction. This design has shown great promise and has been successfully commercialized [264]. This design is recommended for co-pyrolysis because the feedstock can be mixed prior to introduction and remains in close contact with each other, maximizing the extent of synergy.

Based on the evaluations of the different technologies (Tables 14 and 16), both the fixed bed and the rotating cone reactor may be recommended for co-pyrolysis due to the high extent of contact between the fuel particles as well as the effective heat transfer that is achieved through these designs. However the fixed bed reactor is used only for laboratory work whereas the rotating cone reactor is a promising design for commercial co-pyrolysis.

4.2.3. *Reactor product recovery*

The choice of pyrolysis reactor and product recovery system depends on the target product. As shown in Table 14 most reactor designs target the oil product; however, the efficient condensation of vapours has long been a difficulty and different collection systems have been reviewed [273]. In general, a cyclone is required to separate oil and char particles followed by a series of cooling stages. Careful design and temperature

control are recommended to avoid blockages.

4.3. Practical implications of co-pyrolysis of torrefied biomass and coal

Although there has been considerable progress in the commercialization of pyrolysis reactors, the technologies are still in the early stages. The main challenges with commercialization include the high capital and operating costs, low heat efficiency and difficulties with handling/storage of biomass as recently reviewed [274]. The commercialization of co-pyrolysis of torrefied biomass and coal may provide some solutions. It is undisputable that the development of co-pyrolysis technologies could ease the transition between fossil-and renewable-based strategies providing a feedstock suitable to the design of actual industrial plants, which are currently being adapted or rethought [275]. Market analysis and domestic policy measures have already been proposed for torrefaction technologies [276]. Adding torrefied biomass could reduce both the feedstock cost and environmental penalties and thus improve profitability [26]. Actual policies for coal and biomass collection and conversion could be easily adapted to co-pyrolysis-derived products as their quality could reach that of existing marketable products.

The field of co-pyrolysis presents various advantages, however a number of obstacles still need to be overcome for advancing the technology to commercial stage. The following areas are recommended for future research:

- Clear limitations exist for the characterization of co-pyrolysis oil, which hinders the industrial community's confidence in the technology. Future studies should focus on effective yet simple characterization strategies.
- The field of co-pyrolysis kinetics is fairly unexplored. Kinetic datasets, which are representative of fundamental chemistry but also robust enough to predict product formation for different reactor systems are required.
- Future research is recommended on the effective integration of torrefaction and pyrolysis technologies to ensure maximum profitability.

5. Conclusion

The co-pyrolysis of torrefied biomass and coal is an attractive process for the thermochemical conversion industry's transition to green energy and products. This review showed how useful it is to understand the effects of operating conditions on the fundamental physico-chemical changes that occur during co-pyrolysis. By studying these changes, it was possible to predict how torrefied biomass might behave differently to raw biomass during co-pyrolysis with coal. The following are key take-home messages of this review:

- To produce a good torrefied material with properties similar to coal, operating temperatures should be selected for the optimal degradation of hemicelluloses (between 225 and 325 °C).
- The differences in physico-chemical properties of raw and torrefied biomass suggest that the extent of heat and mass transfer limitations during co-pyrolysis of coal with torrefied biomass are reduced.
- Insights in co-pyrolysis chemistry reveal the role played by H-donors from biomass to prevent recombination reactions in coal and the catalytic effects of AAEM in biomass. Although torrefied biomass contains less H-donors, the increased activity of surface sites, such as metallic oxides, may lead to increased catalytic effects during co-pyrolysis.
- State-of-the-art co-pyrolysis kinetic relations are based on an additive approach and increased research efforts are clearly required in this field.
- Heat transfer is crucial in co-pyrolysis reactors and the contribution of different mechanisms of heat transfer strongly depends on the reactor configuration. Although fluidized bed reactors have been suggested, serious problems with up-scaling are experienced. The rotating cone reactor is suggested as a more promising technology for co-pyrolysis commercialization.

Declaration of competing interest

The authors declare that they have no known competing financial interests or personal relationships that could have appeared to influence the work reported in this paper.

Acknowledgements

This work was financially supported by the National Research Foundation (NRF) [Coal Research Chair Grant No. 86880] and Sasol. Opinions, findings and conclusions or recommendations expressed in any publication generated by the NRF supported research are that of the author(s) alone, and that the NRF accepts no liability whatsoever in this regard.

The authors also acknowledges the French scientific program MOPGA (reference ANR-18-MPGA-0013) managed by the National Research Agency and financially supported by the "Investissements d'Avenir.

Appendix A. Supplementary data

Supplementary data to this article can be found online at https://doi.org/10.1016/j.rser.2020.110189.

References

[1] Chu S, Majumdar A. Opportunities and challenges for a sustainable energy future. Nature 2012;488:294.
[2] Administration USEI. International energy outlook. 2017. https://www.eia.gov/outlooks/ieo/pdf/0484(2017).pdf. [Accessed 19 March 2018].
[3] Patel M, Zhang X, Kumar A. Techno-economic and life cycle assessment on lignocellulosic biomass thermochemical conversion technologies: a review. Renew Sustain Energy Rev 2016;53:1486–99.
[4] Agency IE. Annual report IEA bioenergy. 2017. http://www.ieabioenergy.com/wp-content/uploads/2018/04/IEA-Bioenergy-Annual-Report-2017.pdf. [Accessed 19 March 2018].
[5] Bridgwater A. Principles and practice of biomass fast pyrolysis processes for liquids. J Anal Appl Pyrol 1999;51:3–22.
[6] Abnisa F, Daud WMAW. A review on co-pyrolysis of biomass: an optional technique to obtain a high-grade pyrolysis oil. Energy Convers Manag 2014;87:71–85.
[7] Bridgwater A, Peacocke G. Fast pyrolysis processes for biomass. Renew Sustain Energy Rev 2000;4:1–73.
[8] Van der Stelt M, Gerhauser H, Kiel J, Ptasinski K. Biomass upgrading by torrefaction for the production of biofuels: a review. Biomass Bioenergy 2011;35:3748–62.
[9] Xue F, Li D, Guo Y, Liu X, Zhang X, Zhou Q, et al. Technical progress and the prospect of low-rank coal pyrolysis in China. Energy Technol 2017;5:1897–907.
[10] Crude Oil Prices - 70 Year Historical Chart. http://www.macrotrends.net/1369/crude-oil-price-history-chart [accessed 10 July 2020].
[11] Demirbaş A. Sustainable cofiring of biomass with coal. Energy Convers Manag 2003;44:1465–79.
[12] Institute SANED. Appraisal of implementation of fossil fuel and renewable energy hybrid technologies in South Africa. 2017.
[13] Weiland NT, Means NC, Morreale BD. Product distributions from isothermal co-pyrolysis of coal and biomass. Fuel 2012;94:563–70.
[14] Yang Z, Wu Y, Zhang Z, Li H, Li X, Egorov RI, et al. Recent advances in co-thermochemical conversions of biomass with fossil fuels focusing on the synergistic effects. Renew Sustain Energy Rev 2019;103:384–98.
[15] Soncini RM, Means NC, Weiland NT. Co-pyrolysis of low rank coals and biomass: product distributions. Fuel 2013;112:74–82.
[16] Quan C, Gao N. Co-pyrolysis of biomass and coal: a review of effects of co-pyrolysis parameters, product properties, and synergistic mechanisms. BioMed Res Int 2016;2016:1–11. 6197867.
[17] Hassan H, Lim J, Hameed B. Recent progress on biomass co-pyrolysis conversion into high-quality bio-oil. Bioresour Technol 2016;221:645–55.
[18] Mushtaq F, Mat R, Ani FN. A review on microwave assisted pyrolysis of coal and biomass for fuel production. Renew Sustain Energy Rev 2014;39:555–74.
[19] Jones J, Kubacki M, Kubica K, Ross A, Williams A. Devolatilisation characteristics of coal and biomass blends. J Anal Appl Pyrol 2005;74:502–11.
[20] Meng J, Park J, Tilotta D, Park S. The effect of torrefaction on the chemistry of fast-pyrolysis bio-oil. Bioresour Technol 2012;111:439–46.

[21] Sharifzadeh M, Sadeqzadeh M, Guo M, Borhani TN, Konda NM, Garcia MC, et al. The multi-scale challenges of biomass fast pyrolysis and bio-oil upgrading: review of the state of art and future research directions. Prog Energy Combust Sci 2019; 71:1–80.
[22] Ru B, Wang S, Dai G, Zhang L. Effect of torrefaction on biomass physicochemical characteristics and the resulting pyrolysis behavior. Energy Fuels 2015;29: 5865–74.
[23] Acharya B, Sule I, Dutta A. A review on advances of torrefaction technologies for biomass processing. Biomass Conversion and Biorefinery 2012;2:349–69.
[24] Chew J, Doshi V. Recent advances in biomass pretreatment–Torrefaction fundamentals and technology. Renew Sustain Energy Rev 2011;15:4212–22.
[25] Chen Z, Wang M, Jiang E, Wang D, Zhang K, Ren Y, et al. Pyrolysis of torrefied biomass. Trends Biotechnol December 2018;36(12):1287–98.
[26] Dai L, Wang Y, Liu Y, Ruan R, He C, Yu Z, et al. Integrated process of lignocellulosic biomass torrefaction and pyrolysis for upgrading bio-oil production: a state-of-the-art review. Renew Sustain Energy Rev 2019;107:20–36.
[27] Mafu LD, Neomagus HW, Everson RC, Carrier M, Strydom CA, Bunt JR. Structural and chemical modifications of typical South African biomasses during torrefaction. Bioresour Technol 2016;202:192–7.
[28] Levine DG, Schlosberg RH, Silbernagel BG. Understanding the chemistry and physics of coal structure (A Review). National Acad Sciences; 1982.
[29] Vassilev SV, Vassileva CG, Vassilev VS. Advantages and disadvantages of composition and properties of biomass in comparison with coal: an overview. Fuel 2015;158:330–50.
[30] Sheng C, Azevedo J. Estimating the higher heating value of biomass fuels from basic analysis data. Biomass Bioenergy 2005;28:499–507.
[31] Vargas-Moreno J, Callejón-Ferre A, Pérez-Alonso J, Velázquez-Martí B. A review of the mathematical models for predicting the heating value of biomass materials. Renew Sustain Energy Rev 2012;16:3065–83.
[32] Masiá AT, Buhre B, Gupta R, Wall T. Characterising ash of biomass and waste. Fuel Process Technol 2007;88:1071–81.
[33] Şensöz S, Can M. Pyrolysis of pine (Pinus brutia Ten.) chips: 1. Effect of pyrolysis temperature and heating rate on the product yields. Energy Sources 2002;24: 347–55.
[34] Garcia-Perez M, Adams TT, Goodrum JW, Geller DP, Das K. Production and fuel properties of pine chip bio-oil/biodiesel blends. Energy Fuels 2007;21:2363–72.
[35] García R, Pizarro C, Lavín AG, Bueno JL. Spanish biofuels heating value estimation. Part II: Proximate analysis data. Fuel 2014;117:1139–47.
[36] García R, Pizarro C, Lavín AG, Bueno JL. Spanish biofuels heating value estimation. Part I: ultimate analysis data. Fuel 2014;117:1130–8.
[37] Tillman DA. Biomass cofiring: the technology, the experience, the combustion consequences. Biomass Bioenergy 2000;19:365–84.
[38] Lunguleasa A, Spirchez C, Griu T. Effects and modeling of sawdust torrefaction for beech pellets. BioResources 2015;10:4726–39.
[39] Wander PR, Altafini CR, Barreto RM. Assessment of a small sawdust gasification unit. Biomass Bioenergy 2004;27:467–76.
[40] Miles TR, Miles Jr T, Baxter L, Bryers R, Jenkins B, Oden L. Alkali deposits found in biomass power plants: a preliminary investigation of their extent and nature, vol. 1. Golden, CO (United States); Miles: National Renewable Energy Lab.; 1995 (Thomas R ….
[41] Worasuwannarak N, Sonobe T, Tanthapanichakoon W. Pyrolysis behaviors of rice straw, rice husk, and corncob by TG-MS technique. J Anal Appl Pyrol 2007;78: 265–71.
[42] Huang Y-F, Chiueh P-T, Shih C-H, Lo S-L, Sun L, Zhong Y, et al. Microwave pyrolysis of rice straw to produce biochar as an adsorbent for CO2 capture. Energy 2015;84:75–82.
[43] Li S, Chen X, Liu A, Wang L, Yu G. Study on co-pyrolysis characteristics of rice straw and Shenfu bituminous coal blends in a fixed bed reactor. Bioresour Technol 2014;155:252–7.
[44] Sutcu H. Pyrolysis by thermogravimetric analysis of blends of peat with coals of different characteristics and biomass. J Chin Inst Chem Eng 2007;38:245–9.
[45] Sutcu H. Pyrolysis of peat: product yield and characterization. Kor J Chem Eng 2007;24:736–41.
[46] Güldoğan Y, Durusoy T, Bozdemir TÖ. Pyrolysis kinetics of blends of Tuncbilek lignite with Denizli peat. Thermochim Acta 1999;332:75–81.
[47] Suuberg EM, Peters WA, Howard JB. Product composition and kinetics of lignite pyrolysis. Ind Eng Chem Process Des Dev 1978;17:37–46.
[48] Méndez L, Borrego A, Martinez-Tarazona M, Menendez R. Influence of petrographic and mineral matter composition of coal particles on their combustion reactivity☆. Fuel 2003;82:1875–82.
[49] Gouws SM, Neomagus HW, Roberts DG, Bunt JR, Everson RC. The effect of carbon dioxide partial pressure on the gasification rate and pore development of Highveld coal chars at elevated pressures. Fuel Process Technol 2018;179:1–9.
[50] Cuiping L, Chuangzhi W, Haitao H. Chemical elemental characteristics of biomass fuels in China. Biomass Bioenergy 2004;27:119–30.
[51] Van Dyk J, Keyser M, Coertzen M. Syngas production from South African coal sources using Sasol–Lurgi gasifiers. Int J Coal Geol 2006;65:243–53.
[52] Arenillas A, Rubiera F, Pis J. Simultaneous thermogravimetric–mass spectrometric study on the pyrolysis behaviour of different rank coals. J Anal Appl Pyrol 1999;50:31–46.
[53] Bratek K, Bratek W, Gerus-Piasecka I, Jasieńko S, Wilk P. Properties and structure of different rank anthracites. Fuel 2002;81:97–108.
[54] Seo DK, Park SS, Hwang J, Yu T-U. Study of the pyrolysis of biomass using thermo-gravimetric analysis (TGA) and concentration measurements of the evolved species. J Anal Appl Pyrol 2010;89:66–73.
[55] Damartzis T, Vamvuka D, Sfakiotakis S, Zabaniotou A. Thermal degradation studies and kinetic modeling of cardoon (Cynara cardunculus) pyrolysis using thermogravimetric analysis (TGA). Bioresour Technol 2011;102:6230–8.
[56] El-Sayed SA, Mostafa M. Pyrolysis characteristics and kinetic parameters determination of biomass fuel powders by differential thermal gravimetric analysis (TGA/DTG). Energy Convers Manag 2014;85:165–72.
[57] Chen W-H, Kuo P-C. A study on torrefaction of various biomass materials and its impact on lignocellulosic structure simulated by a thermogravimetry. Energy 2010;35:2580–6.
[58] Carrier M, Loppinet-Serani A, Denux D, Lasnier J-M, Ham-Pichavant F, Cansell F, et al. Thermogravimetric analysis as a new method to determine the lignocellulosic composition of biomass. Biomass Bioenergy 2011;35:298–307.
[59] Vhathvarothai N, Ness J, Yu QJ. An investigation of thermal behaviour of biomass and coal during copyrolysis using thermogravimetric analysis. Int J Energy Res 2014;38:1145–54.
[60] Ren S, Lei H, Wang L, Bu Q, Chen S, Wu J. Thermal behaviour and kinetic study for woody biomass torrefaction and torrefied biomass pyrolysis by TGA. Biosyst Eng 2013;116:420–6.
[61] Doddapaneni TRKC, Konttinen J, Hukka TI, Moilanen A. Influence of torrefaction pretreatment on the pyrolysis of Eucalyptus clone: a study on kinetics, reaction mechanism and heat flow. Ind Crop Prod 2016;92:244–54.
[62] Wannapeera J, Fungtammasan B, Worasuwannarak N. Effects of temperature and holding time during torrefaction on the pyrolysis behaviors of woody biomass. J Anal Appl Pyrol 2011;92:99–105.
[63] Lu K-M, Lee W-J, Chen W-H, Lin T-C. Thermogravimetric analysis and kinetics of co-pyrolysis of raw/torrefied wood and coal blends. Appl Energy 2013;105: 57–65.
[64] White JE, Catallo WJ, Legendre BL. Biomass pyrolysis kinetics: a comparative critical review with relevant agricultural residue case studies. J Anal Appl Pyrol 2011;91:1–33.
[65] Collot A-G, Zhuo Y, Dugwell D, Kandiyoti R. Co-pyrolysis and co-gasification of coal and biomass in bench-scale fixed-bed and fluidised bed reactors. Fuel 1999; 78:667–79.
[66] Wang J, Yan Q, Zhao J, Wang Z, Huang J, Gao S, et al. Fast co-pyrolysis of coal and biomass in a fluidized-bed reactor. J Therm Anal Calorim 2014;118:1663–73.
[67] Mao Y, Dong L, Dong Y, Liu W, Chang J, Yang S, et al. Fast co-pyrolysis of biomass and lignite in a micro fluidized bed reactor analyzer. Bioresour Technol 2015; 181:155–62.
[68] Moghtaderi B, Meesri C, Wall TF. Pyrolytic characteristics of blended coal and woody biomass. Fuel 2004;83:745–50.
[69] Li S, Chen X, Wang L, Liu A, Yu G. Co-pyrolysis behaviors of saw dust and Shenfu coal in drop tube furnace and fixed bed reactor. Bioresour Technol 2013;148: 24–9.
[70] Zhang L, Xu S, Zhao W, Liu S. Co-pyrolysis of biomass and coal in a free fall reactor. Fuel 2007;86:353–9.
[71] Wu Z, Wang S, Zhao J, Chen L, Meng H. Product distribution during co-pyrolysis of bituminous coal and lignocellulosic biomass major components in a drop-tube furnace. Energy Fuels 2015;29:4168–80.
[72] Wei L-g, Zhang L, Xu S-p. Effects of feedstock on co-pyrolysis of biomass and coal in a free-fall reactor. J Fuel Chem Technol 2011;39:728–34.
[73] Quan C, Xu S, An Y, Liu X. Co-pyrolysis of biomass and coal blend by TG and in a free fall reactor. J Therm Anal Calorim 2014;117:817–23.
[74] Yuan S, Dai Z-h, Zhou Z-j, Chen X-l, Yu G-s, Wang F-c. Rapid co-pyrolysis of rice straw and a bituminous coal in a high-frequency furnace and gasification of the residual char. Bioresour Technol 2012;109:188–97.
[75] Krerkkaiwan S, Fushimi C, Tsutsumi A, Kuchonthara P. Synergetic effect during co-pyrolysis/gasification of biomass and sub-bituminous coal. Fuel Process Technol 2013;115:11–8.
[76] Yılgın M, Duranay ND, Pehlivan D. Co-pyrolysis of lignite and sugar beet pulp. Energy Convers Manag 2010;51:1060–4.
[77] Guo M, Bi J-C. Characteristics and application of co-pyrolysis of coal/biomass blends with solid heat carrier. Fuel Process Technol 2015;138:743–9.
[78] Song Y, Tahmasebi A, Yu J. Co-pyrolysis of pine sawdust and lignite in a thermogravimetric analyzer and a fixed-bed reactor. Bioresour Technol 2014; 174:204–11.
[79] Aboyade AO, Carrier M, Meyer EL, Knoetze H, Görgens JF. Slow and pressurized co-pyrolysis of coal and agricultural residues. Energy Convers Manag 2013;65: 198–207.
[80] Zhao H, Song Q, Liu S, Li Y, Wang X, Shu X. Study on catalytic co-pyrolysis of physical mixture/staged pyrolysis characteristics of lignite and straw over an catalytic beds of char and its mechanism. Energy Convers Manag 2018;161: 13–26.
[81] Park DK, Kim SD, Lee SH, Lee JG. Co-pyrolysis characteristics of sawdust and coal blend in TGA and a fixed bed reactor. Bioresour Technol 2010;101:6151–6.
[82] Yang X, Yuan C, Xu J, Zhang W. Co-pyrolysis of Chinese lignite and biomass in a vacuum reactor. Bioresour Technol 2014;173:1–5.
[83] Wang M, Tian J, Roberts DG, Chang L, Xie K. Interactions between corncob and lignite during temperature-programmed co-pyrolysis. Fuel 2015;142:102–8.
[84] Meesri C, Moghtaderi B. Lack of synergetic effects in the pyrolytic characteristics of woody biomass/coal blends under low and high heating rate regimes. Biomass Bioenergy 2002;23:55–66.
[85] Ö Onay, Bayram E, Koçkar ÖM. Copyrolysis of seyitömer– lignite and safflower seed: influence of the blending ratio and pyrolysis temperature on product yields and oil characterization. Energy Fuels 2007;21:3049–56.

[86] Vyazovkin S, Burnham AK, Criado JM, Pérez-Maqueda LA, Popescu C, Sbirrazzuoli N. ICTAC Kinetics Committee recommendations for performing kinetic computations on thermal analysis data. Thermochim Acta 2011;520:1–19.
[87] Pan YG, Velo E, Puigjaner L. Pyrolysis of blends of biomass with poor coals. Fuel 1996;75:412–8.
[88] Biagini E, Lippi F, Petarca L, Tognotti L. Devolatilization rate of biomasses and coal–biomass blends: an experimental investigation. Fuel 2002;81:1041–50.
[89] Kastanaki E, Vamvuka D, Grammelis P, Kakaras E. Thermogravimetric studies of the behavior of lignite–biomass blends during devolatilization. Fuel Process Technol 2002;77:159–66.
[90] Vamvuka D, Kakaras E, Kastanaki E, Grammelis P. Pyrolysis characteristics and kinetics of biomass residuals mixtures with lignite☆. Fuel 2003;82:1949–60.
[91] Vuthaluru HB. Thermal behaviour of coal/biomass blends during co-pyrolysis. Fuel Process Technol 2003;85:141–55.
[92] Biagini E, Barontini F, Tognotti L. Devolatilization of biomass fuels and biomass components studied by TG/FTIR technique. Ind Eng Chem Res 2006;45:4486–93.
[93] Sonobe T, Worasuwannarak N, Pipatmanomai S. Synergies in co-pyrolysis of Thai lignite and corncob. Fuel Process Technol 2008;89:1371–8.
[94] Sadhukhan AK, Gupta P, Goyal T, Saha RK. Modelling of pyrolysis of coal-biomass blends using thermogravimetric analysis. Bioresour Technol 2008;99:8022–6.
[95] Ulloa CA, Gordon AL, García XA. Thermogravimetric study of interactions in the pyrolysis of blends of coal with radiata pine sawdust. Fuel Process Technol 2009;90:583–90.
[96] Idris SS, Abd Rahman N, Ismail K, Alias AB, Abd Rashid Z, Aris MJ. Investigation on thermochemical behaviour of low rank Malaysian coal, oil palm biomass and their blends during pyrolysis via thermogravimetric analysis (TGA). Bioresour Technol 2010;101:4584–92.
[97] Di Nola G, de Jong W, Spliethoff H. TG-FTIR characterization of coal and biomass single fuels and blends under slow heating rate conditions: partitioning of the fuel-bound nitrogen. Fuel Process Technol 2010;91:103–15.
[98] Haykiri-Acma H, Yaman S. Interaction between biomass and different rank coals during co-pyrolysis. Renew Energy 2010;35:288–92.
[99] Wang J, Zhang S-y, Guo X, Dong A-x, Chen C, Xiong S-w, et al. Thermal behaviors and kinetics of pingshuo coal/biomass blends during copyrolysis and cocombustion. Energy Fuels 2012;26:7120–6.
[100] Aboyade AO, Carrier M, Meyer EL, Knoetze JH, Görgens JF. Model fitting kinetic analysis and characterisation of the devolatilization of coal blends with corn and sugarcane residues. Thermochim Acta 2012;530:95–106.
[101] Chen C, Ma X, He Y. Co-pyrolysis characteristics of microalgae Chlorella vulgaris and coal through TGA. Bioresour Technol 2012;117:264–73.
[102] Ferrara F, Orsini A, Plaisant A, Pettinau A. Pyrolysis of coal, biomass and their blends: performance assessment by thermogravimetric analysis. Bioresour Technol 2014;171:433–41.
[103] Masnadi MS, Habibi R, Kopyscinski J, Hill JM, Bi X, Lim CJ, et al. Fuel characterization and co-pyrolysis kinetics of biomass and fossil fuels. Fuel 2014;117:1204–14.
[104] Wu Z, Wang S, Zhao J, Chen L, Meng H. Thermal behavior and char structure evolution of bituminous coal blends with edible fungi residue during Co-pyrolysis. Energy Fuels 2014;28:1792–801.
[105] Jeong HM, Seo MW, Jeong SM, Na BK, Yoon SJ, Lee JG, et al. Pyrolysis kinetics of coking coal mixed with biomass under non-isothermal and isothermal conditions. Bioresour Technol 2014;155:442–5.
[106] Agarwal G, Lattimer B. Physicochemical, kinetic and energetic investigation of coal–biomass mixture pyrolysis. Fuel Process Technol 2014;124:174–87.
[107] Li S, Chen X, Liu A, Wang L, Yu G. Co-pyrolysis characteristic of biomass and bituminous coal. Bioresour Technol 2015;179:414–20.
[108] Meng H, Wang S, Chen L, Wu Z, Zhao J. Thermal behavior and the evolution of char structure during co-pyrolysis of platanus wood blends with different rank coals from northern China. Fuel 2015;158:602–11.
[109] Guan Y, Ma Y, Zhang K, Chen H, Xu G, Liu W, et al. Co-pyrolysis behaviors of energy grass and lignite. Energy Convers Manag 2015;93:132–40.
[110] Montiano MG, Diaz-Faes E, Barriocanal C. Kinetics of co-pyrolysis of sawdust, coal and tar. Bioresour Technol 2016;205:222–9.
[111] Wu Z, Wang S, Zhao J, Chen L, Meng H. Thermochemical behavior and char morphology analysis of blended bituminous coal and lignocellulosic biomass model compound co-pyrolysis: effects of cellulose and carboxymethylcellulose sodium. Fuel 2016;171:65–73.
[112] Zhang Y, Fan D, Zheng Y. Comparative study on combined co-pyrolysis/gasification of walnut shell and bituminous coal by conventional and congruent-mass thermogravimetric analysis (TGA) methods. Bioresour Technol 2016;199:382–5.
[113] Saikia M, Ali AA, Borah RC, Bezbarua MS, Saikia BK, Saikia N. Effects of biomass types on the co-pyrolysis behaviour of a sub-bituminous high-sulphur coal. Energy, Ecology and Environment 2018;3:251–65.
[114] Qiu S, Zhang S, Zhou X, Zhang Q, Qiu G, Hu M, et al. Thermal behavior and organic functional structure of poplar-fat coal blends during co-pyrolysis. Renew Energy 2019;136:308–16.
[115] Grønli M, Antal MJ, Varhegyi G. A round-robin study of cellulose pyrolysis kinetics by thermogravimetry. Ind Eng Chem Res 1999;38:2238–44.
[116] Narayan R, Antal MJ. Thermal lag, fusion, and the compensation effect during biomass pyrolysis. Ind Eng Chem Res 1996;35:1711–21.
[117] SR, Volker Th. Thermokinetic investigation of cellulose pyrolysis. 2002.
[118] He Q, Ding L, Gong Y, Li W, Wei J, Yu G. Effect of torrefaction on pinewood pyrolysis kinetics and thermal behavior using thermogravimetric analysis. Bioresour Technol 2019;280:104–11.
[119] Völker S, Rieckmann T. Thermokinetic investigation of cellulose pyrolysis—impact of initial and final mass on kinetic results. J Anal Appl Pyrol 2002;62:165–77.
[120] Granados D, Chejne F, Basu P. A two dimensional model for torrefaction of large biomass particles. J Anal Appl Pyrol 2016;120:1–14.
[121] Grønli MG, Melaaen MC. Mathematical model for wood pyrolysis comparison of experimental measurements with model predictions. Energy Fuels 2000;14:791–800.
[122] Rousset P, Perré P, Girard P. Modification of mass transfer properties in poplar wood (P. robusta) by a thermal treatment at high temperature. Holz als Roh-und Werkstoff 2004;62:113–9.
[123] Mafu LD, Neomagus HW, Everson RC, Strydom CA, Carrier M, Okolo GN, et al. Chemical and structural characterization of char development during lignocellulosic biomass pyrolysis. Bioresour Technol 2017;243:941–8.
[124] Antal MJJ, Varhegyi G. Cellulose pyrolysis kinetics: the current state of knowledge. Ind Eng Chem Res 1995;34:703–17.
[125] Pyle D, Zaror C. Heat transfer and kinetics in the low temperature pyrolysis of solids. Chem Eng Sci 1984;39:147–58.
[126] Di Blasi C. Kinetic and heat transfer control in the slow and flash pyrolysis of solids. Ind Eng Chem Res 1996;35:37–46.
[127] Lédé J, Authier O. Temperature and heating rate of solid particles undergoing a thermal decomposition. Which criteria for characterizing fast pyrolysis? J Anal Appl Pyrol 2015;113:1–14.
[128] Mason P, Darvell L, Jones J, Williams A. Comparative study of the thermal conductivity of solid biomass fuels. Energy Fuels 2016;30:2158–63.
[129] Shen J, Igathinathane C, Yu M, Pothula AK. Biomass pyrolysis and combustion integral and differential reaction heats with temperatures using thermogravimetric analysis/differential scanning calorimetry. Bioresour Technol 2015;185:89–98.
[130] Larraín T, Carrier M, Radovic LR. Structure-reactivity relationship in pyrolysis of plastics: a comparison with natural polymers. J Anal Appl Pyrol 2017;126:346–56.
[131] He Q, Guo Q, Ding L, Gong Y, Wei J, Yu G. Co-pyrolysis behavior and char structure evolution of raw/torrefied rice straw and coal blends. Energy & Fuels; 2018.
[132] Aboyade AO, Görgens JF, Carrier M, Meyer EL, Knoetze JH. Thermogravimetric study of the pyrolysis characteristics and kinetics of coal blends with corn and sugarcane residues. Fuel Process Technol 2013;106:310–20.
[133] Stiller AH, Dadyburjor DB, Wann J-P, Tian D, Zondlo JW. Co-processing of agricultural and biomass waste with coal. Fuel Process Technol 1996;49:167–75.
[134] Solomon PR, Serio MA, Suuberg EM. Coal pyrolysis: experiments, kinetic rates and mechanisms. Prog Energy Combust Sci 1992;18:133–220.
[135] Wang Y-J, Ying H, Sun Y-J, Jiang J-F, Jiang J-C, Gao Y-W, et al. Co-pyrolysis characteristics of torrefied pine sawdust with different rank coals. BioResources 2013;8:5169–83.
[136] Vassilev SV, Baxter D, Andersen LK, Vassileva CG, Morgan TJ. An overview of the organic and inorganic phase composition of biomass. Fuel 2012;94:1–33.
[137] Mettler MS, Vlachos DG, Dauenhauer PJ. Top ten fundamental challenges of biomass pyrolysis for biofuels. Energy Environ Sci 2012;5:7797–809.
[138] Mamleev V, Bourbigot S, Le Bras M, Yvon J. The facts and hypotheses relating to the phenomenological model of cellulose pyrolysis: interdependence of the steps. J Anal Appl Pyrol 2009;84:1–17.
[139] Raveendran K, Ganesh A, Khilar KC. Influence of mineral matter on biomass pyrolysis characteristics. Fuel 1995;74:1812–22.
[140] He Y, Zhai Y, Li C, Yang F, Chen L, Fan X, et al. The fate of Cu, Zn, Pb and Cd during the pyrolysis of sewage sludge at different temperatures. Environ Technol 2010;31:567–74.
[141] Patwardhan PR, Satrio JA, Brown RC, Shanks BH. Influence of inorganic salts on the primary pyrolysis products of cellulose. Bioresour Technol 2010;101:4646–55.
[142] Weber K, Quicker P. Properties of biochar. Fuel 2018;217:240–61.
[143] Trubetskaya A, Leahy JJ, Yazhenskikh E, Müller M, Layden P, Johnson R, et al. Characterization of woodstove briquettes from torrefied biomass and coal. Energy 2019;171:853–65.
[144] Kim Y-H, Lee S-M, Lee H-W, Lee J-W. Physical and chemical characteristics of products from the torrefaction of yellow poplar (Liriodendron tulipifera). Bioresour Technol 2012;116:120–5.
[145] Khazraie Shoulaifar T, DeMartini N, Zevenhoven M, Verhoeff F, Kiel J, Hupa M. Ash-forming matter in torrefied birch wood: changes in chemical association. Energy Fuels 2013;27:5684–90.
[146] Leijenhorst EJ, Wolters W, Van De Beld L, Prins W. Inorganic element transfer from biomass to fast pyrolysis oil: review and experiments. Fuel Process Technol 2016;149:96–111.
[147] Zhang Y, Geng P, Liu R. Synergistic combination of biomass torrefaction and co-gasification: reactivity studies. Bioresour Technol 2017;245:225–33.
[148] Ren S, Lei H, Wang L, Bu Q, Chen S, Wu J. Hydrocarbon and hydrogen-rich syngas production by biomass catalytic pyrolysis and bio-oil upgrading over biochar catalysts. RSC Adv 2014;4:10731–7.
[149] Feng D, Zhao Y, Zhang Y, Sun S, Meng S, Guo Y, et al. Effects of K and Ca on reforming of model tar compounds with pyrolysis biochars under H2O or CO2. Chem Eng J 2016;306:422–32.
[150] Collard F-X, Carrier M, Görgens J. Fractionation of lignocellulosic material with pyrolysis processing. Biomass fractionation technologies for a lignocellulosic feedstock based biorefinery. Elsevier; 2016. p. 81–101.

[151] Neves D, Thunman H, Matos A, Tarelho L, Gómez-Barea A. Characterization and prediction of biomass pyrolysis products. Prog Energy Combust Sci 2011;37:611–30.
[152] Garcia-Perez M, Wang XS, Shen J, Rhodes MJ, Tian F, Lee W-J, et al. Fast pyrolysis of oil mallee woody biomass: effect of temperature on the yield and quality of pyrolysis products. Ind Eng Chem Res 2008;47:1846–54.
[153] Cui L-j, Lin W-g, Yoa J-z. Influences of temperature and coal particle size on the flash pyrolysis of coal in a fast-entrained bed. Chem Res Chin Univ 2006;22:103–10.
[154] Morf P, Hasler P, Nussbaumer T. Mechanisms and kinetics of homogeneous secondary reactions of tar from continuous pyrolysis of wood chips. Fuel 2002;81:843–53.
[155] Song Y, Tahmasebi A, Yu J. Co-pyrolysis of pine sawdust and lignite in a thermogravimetric analyzer and a fixed-bed reactor. Bioresour Technol 2014;174:204–11.
[156] Zheng A, Zhao Z, Chang S, Huang Z, He F, Li H. Effect of torrefaction temperature on product distribution from two-staged pyrolysis of biomass. Energy Fuels 2012;26:2968–74.
[157] Mok WS-L, Antal Jr MJ. Effects of pressure on biomass pyrolysis. I. Cellulose pyrolysis products. Thermochim Acta 1983;68:155–64.
[158] Chen H, Luo Z, Yang H, Ju F, Zhang S. Pressurized pyrolysis and gasification of Chinese typical coal samples. Energy Fuels 2008;22:1136–41.
[159] Huang Y, Wang N, Liu Q, Wang W, Ma X. Co-pyrolysis of bituminous coal and biomass in a pressured fluidized bed. Chin J Chem Eng July 2019;27(7):1666–73.
[160] Carrier M, Hugo T, Gorgens J, Knoetze H. Comparison of slow and vacuum pyrolysis of sugar cane bagasse. J Anal Appl Pyrol 2011;90:18–26.
[161] Sathe C, Hayashi J-I, Li C-Z. Release of volatiles from the pyrolysis of a Victorian lignite at elevated pressures. Fuel 2002;81:1171–8.
[162] Wafiq A, Reichel D, Hanafy M. Pressure influence on pyrolysis product properties of raw and torrefied Miscanthus: role of particle structure. Fuel 2016;179:156–67.
[163] Qian Y, Zhang J, Wang J. Pressurized pyrolysis of rice husk in an inert gas sweeping fixed-bed reactor with a focus on bio-oil deoxygenation. Bioresour Technol 2014;174:95–102.
[164] Collard F-X, Blin J. A review on pyrolysis of biomass constituents: mechanisms and composition of the products obtained from the conversion of cellulose, hemicelluloses and lignin. Renew Sustain Energy Rev 2014;38:594–608.
[165] Scaroni AW, Khan MR, Eser S, Radovic LR. Coal pyrolysis. Ullmann's encyclopedia of industrial chemistry. sixth ed. Wiley-VCH Verlag GmbH & Co. KGaA; 1986. p. 719–54.
[166] Chen W-H, Lu K-M, Tsai C-M. An experimental analysis on property and structure variations of agricultural wastes undergoing torrefaction. Appl Energy 2012;100:318–25.
[167] Azargohar R, Nanda S, Kozinski JA, Dalai AK, Sutarto R. Effects of temperature on the physicochemical characteristics of fast pyrolysis bio-chars derived from Canadian waste biomass. Fuel 2014;125:90–100.
[168] Fu P, Hu S, Sun L, Xiang J, Yang T, Zhang A, et al. Structural evolution of maize stalk/char particles during pyrolysis. Bioresour Technol 2009;100:4877–83.
[169] Chen Y, Zhang X, Chen W, Yang H, Chen H. The structure evolution of biochar from biomass pyrolysis and its correlation with gas pollutant adsorption performance. Bioresour Technol 2017;246:101–9.
[170] Li T, Zhang L, Dong L, Qiu P, Wang S, Jiang S, et al. Changes in char structure during the low-temperature pyrolysis in N2 and subsequent gasification in air of Loy Yang brown coal char. Fuel 2018;212:187–92.
[171] Le Brech Y, Raya J, Delmotte L, Brosse N, Gadiou R, Dufour A. Characterization of biomass char formation investigated by advanced solid state NMR. Carbon 2016;108:165–77.
[172] Anca-Couce A. Reaction mechanisms and multi-scale modelling of lignocellulosic biomass pyrolysis. Prog Energy Combust Sci 2016;53:41–79.
[173] Wu Z, Yang W, Chen L, Meng H, Zhao J, Wang S. Morphology and microstructure of co-pyrolysis char from bituminous coal blended with lignocellulosic biomass: effects of cellulose, hemicellulose and lignin. Appl Therm Eng 2017;116:24–32.
[174] Keown DM, Li X, Hayashi J-i, Li C-Z. Characterization of the structural features of char from the pyrolysis of cane trash using Fourier Transform– Raman spectroscopy. Energy Fuels 2007;21:1816–21.
[175] Zhang S, Hu B, Zhang L, Xiong Y. Effects of torrefaction on yield and quality of pyrolysis char and its application on preparation of activated carbon. J Anal Appl Pyrol 2016;119:217–23.
[176] Fengel D, Wegener G. Wood: chemistry, ultrastructure, reactions. New York: Walter de Gruyter; 1984.
[177] Wang L, Barta-Rajnai E, Ø Skreiberg, Khalil R, Czégény Z, Jakab E, et al. Effect of torrefaction on physiochemical characteristics and grindability of stem wood, stump and bark. Appl Energy 2018;227:137–48.
[178] Chen Y, Liu B, Yang H, Yang Q, Chen H. Evolution of functional groups and pore structure during cotton and corn stalks torrefaction and its correlation with hydrophobicity. Fuel 2014;137:41–9.
[179] Chen H, Chen X, Qin Y, Wei J, Liu H. Effect of torrefaction on the properties of rice straw high temperature pyrolysis char: pore structure, aromaticity and gasification activity. Bioresour Technol 2017;228:241–9.
[180] Jendoubi N, Broust F, Commandre J-M, Mauviel G, Sardin M, Lede J. Inorganics distribution in bio oils and char produced by biomass fast pyrolysis: the key role of aerosols. J Anal Appl Pyrol 2011;92:59–67.
[181] Bridgwater AV. Review of fast pyrolysis of biomass and product upgrading. Biomass Bioenergy 2012;38:68–94.
[182] Lyu G, Wu S, Zhang H. Estimation and comparison of bio-oil components from different pyrolysis conditions. Frontiers in Energy Research 2015;3:28.
[183] Cai W, Liu Q, Shen D, Wang J. Py-GC/MS analysis on product distribution of two-staged biomass pyrolysis. J Anal Appl Pyrol 2019;138:62–9.
[184] Zhang Q, Chang J, Wang T, Xu Y. Review of biomass pyrolysis oil properties and upgrading research. Energy Convers Manag 2007;48:87–92.
[185] Chen Y, Yang H, Yang Q, Hao H, Zhu B, Chen H. Torrefaction of agriculture straws and its application on biomass pyrolysis poly-generation. Bioresour Technol 2014;156:70–7.
[186] Louwes AC, Basile L, Yukananto R, Bhagwandas J, Bramer EA, Brem G. Torrefied biomass as feed for fast pyrolysis: an experimental study and chain analysis. Biomass Bioenergy 2017;105:116–26.
[187] Bridgwater AV. Upgrading biomass fast pyrolysis liquids. Environ Prog Sustain Energy 2012;31:261–8.
[188] Boateng A, Mullen C. Fast pyrolysis of biomass thermally pretreated by torrefaction. J Anal Appl Pyrol 2013;100:95–102.
[189] Fardhyanti D, Damayanti A. Analysis of coal tar compositions produced from sub-bituminous kalimantan coal tar. World academy of science, engineering and technology. International Journal of Chemical, Molecular, Nuclear, Materials and Metallurgical Engineering 2015;9:1022–5.
[190] Mellin P, Kantarelis E, Yang W. Computational fluid dynamics modeling of biomass fast pyrolysis in a fluidized bed reactor, using a comprehensive chemistry scheme. Fuel 2014;117:704–15.
[191] Xue Q, Heindel T, Fox R. A CFD model for biomass fast pyrolysis in fluidized-bed reactors. Chem Eng Sci 2011;66:2440–52.
[192] Vyazovkin S, Wight CA. Isothermal and non-isothermal kinetics of thermally stimulated reactions of solids. Int Rev Phys Chem 1998;17:407–33.
[193] Naqvi SR, Hameed Z, Tariq R, Taqvi SA, Ali I, Niazi MBK, et al. Synergistic effect on co-pyrolysis of rice husk and sewage sludge by thermal behavior, kinetics, thermodynamic parameters and artificial neural network. Waste Manag 2019;85:131–40.
[194] Wang Z, Wan K, Xia J, He Y, Liu Y, Liu J. Pyrolysis characteristics of coal, biomass, and coal–biomass blends under high heating rate conditions: effects of particle diameter, fuel type, and mixing conditions. Energy Fuels 2015;29:5036–46.
[195] Varhegyi G, Antal Jr MJ, Jakab E, Szabó P. Kinetic modeling of biomass pyrolysis. J Anal Appl Pyrol 1997;42:73–87.
[196] Alonso M, Alvarez D, Borrego A, Menéndez R, Marbán G. Systematic effects of coal rank and type on the kinetics of coal pyrolysis. Energy Fuels 2001;15:413–28.
[197] Cai J, Wu W, Liu R. An overview of distributed activation energy model and its application in the pyrolysis of lignocellulosic biomass. Renew Sustain Energy Rev 2014;36:236–46.
[198] Shen D, Gu S, Jin B, Fang M. Thermal degradation mechanisms of wood under inert and oxidative environments using DAEM methods. Bioresour Technol 2011;102:2047–52.
[199] Yan J, Liu M, Feng Z, Bai Z, Shui H, Li Z, et al. Study on the pyrolysis kinetics of low-medium rank coals with distributed activation energy model. Fuel 2020;261:116359.
[200] Chen X, Liu L, Zhang L, Zhao Y, Zhang Z, Xie X, et al. Thermogravimetric analysis and kinetics of the co-pyrolysis of coal blends with corn stalks. Thermochim Acta 2018;659:59–65.
[201] Ranzi E, Cuoci A, Faravelli T, Frassoldati A, Migliavacca G, Pierucci S, et al. Chemical kinetics of biomass pyrolysis. Energy Fuels 2008;22:4292–300.
[202] Bach Q-V, Trinh TN, Tran K-Q, Thi NBD. Pyrolysis characteristics and kinetics of biomass torrefied in various atmospheres. Energy Convers Manag 2017;141:72–8.
[203] Stark SM, Neurock M, Klein MT. Strategies for modelling kinetic interactions in complex mixtures: Monte Carlo algorithms for MIMD parallel architectures. Chem Eng Sci 1993;48:4081–96.
[204] Lin Y, Tian Y, Xia Y, Fang S, Liao Y, Yu Z, et al. General distributed activation energy model (G-DAEM) on co-pyrolysis kinetics of bagasse and sewage sludge. Bioresour Technol 2019;273:545–55.
[205] Zhang L, Liu R, Yin R, Mei Y. Upgrading of bio-oil from biomass fast pyrolysis in China: a review. Renew Sustain Energy Rev 2013;24:66–72.
[206] Mostafazadeh AK, Solomatnikova O, Drogui P, Tyagi RD. A review of recent research and developments in fast pyrolysis and bio-oil upgrading. Biomass Conversion and Biorefinery 2018;8:739–73.
[207] Harmsen P, Huijgen W, Bermudez L, Bakker R. Literature review of physical and chemical pretreatment processes for lignocellulosic biomass. Wageningen UR-Food & Biobased Research; 2010.
[208] Zhu JY, Pan X, Zalesny RS. Pretreatment of woody biomass for biofuel production: energy efficiency, technologies, and recalcitrance. Appl Microbiol Biotechnol 2010;87:847–57.
[209] Carvalheiro F, Duarte LC, Gírio FM. Hemicellulose biorefineries: a review on biomass pretreatments. J Sci Ind Res 2008:849–64.
[210] Nanda S, Mohammad J, Reddy SN, Kozinski JA, Dalai AK. Pathways of lignocellulosic biomass conversion to renewable fuels. Biomass Conversion and Biorefinery 2014;4:157–91.
[211] Alvira P, Tomás-Pejó E, Ballesteros M, Negro M. Pretreatment technologies for an efficient bioethanol production process based on enzymatic hydrolysis: a review. Bioresour Technol 2010;101:4851–61.
[212] Phanphanich M, Mani S. Impact of torrefaction on the grindability and fuel characteristics of forest biomass. Bioresour Technol 2011;102:1246–53.
[213] Peksa M, Dolzan P, Grassi A, Heinimö J, Junginger H, Ranta T-M, et al. Global wood pellets markets and industry: policy drivers, market status and raw material potential. Utrecht University; 2007.

[214] Samuelsson R, Thyrel M, Sjöström M, Lestander TA. Effect of biomaterial characteristics on pelletizing properties and biofuel pellet quality. Fuel Process Technol 2009;90:1129–34.
[215] Stolarski MJ, Szczukowski S, Tworkowski J, Krzyżaniak M, Gulczyński P, Mleczek M. Comparison of quality and production cost of briquettes made from agricultural and forest origin biomass. Renew Energy 2013;57:20–6.
[216] Kaltschmitt M, Weber M. Markets for solid biofuels within the EU-15. Biomass Bioenergy 2006;30:897–907.
[217] Holm JK, Stelte W, Posselt D, Ahrenfeldt J, Henriksen UB. Optimization of a multiparameter model for biomass pelletization to investigate temperature dependence and to facilitate fast testing of pelletization behavior. Energy Fuels 2011;25:3706–11.
[218] Saleh SB, Dam-Johansen K, Jensen PA, Hansen BB. Torrefaction of biomass for power production. 2013.
[219] Cai J, He Y, Yu X, Banks SW, Yang Y, Zhang X, et al. Review of physicochemical properties and analytical characterization of lignocellulosic biomass. Renew Sustain Energy Rev 2017;76:309–22.
[220] Bychkov A, Podgorbunskikh E, Bychkova E, Lomovsky O. Current achievements in the mechanically pretreated conversion of plant biomass. Biotechnology and bioengineering; 2019.
[221] Chen W-H, Peng J, Bi XT. A state-of-the-art review of biomass torrefaction, densification and applications. Renew Sustain Energy Rev 2015;44:847–66.
[222] Nunes L, Matias J, Catalão J. A review on torrefied biomass pellets as a sustainable alternative to coal in power generation. Renew Sustain Energy Rev 2014;40:153–60.
[223] Arias B, Pevida C, Fermoso J, Plaza M, Rubiera F, Pis J. Influence of torrefaction on the grindability and reactivity of woody biomass. Fuel Process Technol 2008;89:169–75.
[224] Tumuluru JS, Wright CT, Boardman RD, Yancey NA, Sokhansanj S. A review on biomass classification and composition, co-firing issues and pretreatment methods. 2011 Louisville, Kentucky, August 7-10, 2011. American Society of Agricultural and Biological Engineers; 2011. p. 1.
[225] Adams P, Shirley J, McManus M. Comparative cradle-to-gate life cycle assessment of wood pellet production with torrefaction. Appl Energy 2015;138:367–80.
[226] Koekemoer A, Luckos A. On the sphericity of coal and char particles. S Afr J Chem Eng 2014;19:62–71.
[227] Tumuluru JS, Sokhansanj S, Hess JR, Wright CT, Boardman RD. A review on biomass torrefaction process and product properties for energy applications. Ind Biotechnol 2011;7:384–401.
[228] Jahirul M, Rasul M, Chowdhury A, Ashwath N. Biofuels production through biomass pyrolysis—a technological review. Energies 2012;5:4952–5001.
[229] Lede J. Biomass fast pyrolysis reactors: a review of a few scientific challenges and of related recommended research topics. Oil & Gas Science and Technology–Revue d'IFP Energies nouvelles 2013;68:801–14.
[230] Tripathi M, Sahu JN, Ganesan P. Effect of process parameters on production of biochar from biomass waste through pyrolysis: a review. Renew Sustain Energy Rev 2016;55:467–81.
[231] Beis S, Ö Onay, Koçkar Ö. Fixed-bed pyrolysis of safflower seed: influence of pyrolysis parameters on product yields and compositions. Renew Energy 2002;26:21–32.
[232] Pütün AE, Özbay N, Önal EP, Pütün E. Fixed-bed pyrolysis of cotton stalk for liquid and solid products. Fuel Process Technol 2005;86:1207–19.
[233] Encinar J, Gonzalez J, Gonzalez J. Fixed-bed pyrolysis of Cynara cardunculus L. Product yields and compositions. Fuel Process Technol 2000;68:209–22.
[234] Kern S, Halwachs M, Kampichler G, Pfeifer C, Pröll T, Hofbauer H. Rotary kiln pyrolysis of straw and fermentation residues in a 3 MW pilot plant–Influence of pyrolysis temperature on pyrolysis product performance. J Anal Appl Pyrol 2012;97:1–10.
[235] Fantozzi F, D'Alessandro B, Bidini G. IPRP (Integrated-Pyrolysis Regenerated Plant): gas turbine and externally heated rotary-kiln pyrolysis as a biomass and waste energy conversion system. Influence of thermodynamic parameters. Proc IME J Power Energy 2003;217:519–27.
[236] Li S-Q, Yao Q, Chi Y, Yan J-H, Cen K-F. Pilot-scale pyrolysis of scrap tires in a continuous rotary kiln reactor. Ind Eng Chem Res 2004;43:5133–45.
[237] Martínez JD, Murillo R, García T, Veses A. Demonstration of the waste tire pyrolysis process on pilot scale in a continuous auger reactor. J Hazard Mater 2013;261:637–45.
[238] Brown JN. Development of a lab-scale auger reactor for biomass fast pyrolysis and process optimization using response surface methodology. 2009.
[239] Solar J, De Marco I, Caballero B, Lopez-Urionabarrenechea A, Rodriguez N, Agirre I, et al. Influence of temperature and residence time in the pyrolysis of woody biomass waste in a continuous screw reactor. Biomass Bioenergy 2016;95:416–23.
[240] Ly HV, Kim S-S, Woo HC, Choi JH, Suh DJ, Kim J. Fast pyrolysis of macroalga Saccharina japonica in a bubbling fluidized-bed reactor for bio-oil production. Energy 2015;93:1436–46.
[241] Xu R, Ferrante L, Briens C, Berruti F. Flash pyrolysis of grape residues into biofuel in a bubbling fluid bed. J Anal Appl Pyrol 2009;86:58–65.
[242] Lee S-H, Eom M-S, Yoo K-S, Kim N-C, Jeon J-K, Park Y-K, et al. The yields and composition of bio-oil produced from Quercus Acutissima in a bubbling fluidized bed pyrolyzer. J Anal Appl Pyrol 2008;83:110–4.
[243] Lappas A, Samolada M, Iatridis D, Voutetakis S, Vasalos I. Biomass pyrolysis in a circulating fluid bed reactor for the production of fuels and chemicals. Fuel 2002;81:2087–95.
[244] Thomsen TP, Sárossy Z, Gøbel B, Stoholm P, Ahrenfeldt J, Frandsen FJ, et al. Low temperature circulating fluidized bed gasification and co-gasification of municipal sewage sludge. Part 1: process performance and gas product characterization. Waste Manag 2017;66:123–33.
[245] Rodjeen S, Mekasut L, Kuchontara P, Piumsomboon P. Parametric studies on catalytic pyrolysis of coal-biomass mixture in a circulating fluidized bed. Kor J Chem Eng 2006;23:216–23.
[246] Zuo W, Jin B, Huang Y, Sun Y, Li R, Jia J. Pyrolysis of high-ash sewage sludge in a circulating fluidized bed reactor for production of liquids rich in heterocyclic nitrogenated compounds. Bioresour Technol 2013;127:44–8.
[247] Ding T, Li S, Xie J, Song W, Yao J, Lin W. Rapid pyrolysis of wheat straw in a bench-scale circulating fluidized-bed downer reactor. Chem Eng Technol 2012;35:2170–6.
[248] Dupont C, Commandre J-M, Gauthier P, Boissonnet G, Salvador S, Schweich D. Biomass pyrolysis experiments in an analytical entrained flow reactor between 1073 K and 1273 K. Fuel 2008;87:1155–64.
[249] Sun S, Tian H, Zhao Y, Sun R, Zhou H. Experimental and numerical study of biomass flash pyrolysis in an entrained flow reactor. Bioresour Technol 2010;101:3678–84.
[250] Morgan ME, Jenkins RG. Pyrolysis of a lignite in an entrained flow reactor: 1. Effect of cations on total weight loss. Fuel 1986;65:757–63.
[251] Westerhout R, Waanders J, Kuipers J, van Swaaij WPM. Development of a continuous rotating cone reactor pilot plant for the pyrolysis of polyethene and polypropene. Ind Eng Chem Res 1998;37:2316–22.
[252] Janse AMC. A heat integrated rotating cone reactor system for flash pyrolysis of biomass. Universiteit Twente; 1998.
[253] Wagenaar B, Prins W, Van Swaaij W. Pyrolysis of biomass in the rotating cone reactor: modelling and experimental justification. Chem Eng Sci 1994;49:5109–26.
[254] Peacocke G, Bridgwater A. Ablative plate pyrolysis of biomass for liquids. Biomass Bioenergy 1994;7:147–54.
[255] Luo G, Eng RJ, Jia P, Resende FL. Ablative pyrolysis of wood chips: effect of operating conditions. Energy Technol 2017;5:2128–37.
[256] Luo G, Chandler DS, Anjos LC, Eng RJ, Jia P, Resende FL. Pyrolysis of whole wood chips and rods in a novel ablative reactor. Fuel 2017;194:229–38.
[257] Dai J, Cui H, Grace JR. Biomass feeding for thermochemical reactors. Prog Energy Combust Sci 2012;38:716–36.
[258] Kenney KL, Smith WA, Gresham GL, Westover TL. Understanding biomass feedstock variability. Biofuels 2013;4:111–27.
[259] Boukis IP, Grammelis P, Bezergianni S, Bridgwater A. CFB air-blown flash pyrolysis. Part I: engineering design and cold model performance. Fuel 2007;86:1372–86.
[260] Whitaker S. Forced convection heat transfer correlations for flow in pipes, past flat plates, single cylinders, single spheres, and for flow in packed beds and tube bundles. AIChE J 1972;18:361–71.
[261] Pandey A, Bhaskar T, Stöcker M, Sukumaran R. Recent advances in thermochemical conversion of biomass. Elsevier; 2015.
[262] Peacocke G, Bridgwater A. Design of a novel ablative pyrolysis reactor. Advances in thermochemical biomass conversion. Springer; 1993. p. 1134–50.
[263] Brown RC. Thermochemical processing of biomass: conversion into fuels, chemicals and power. John Wiley & Sons; 2019.
[264] Venderbosch R, Prins W. Fast pyrolysis technology development. Biofuels, bioproducts and biorefining 2010;4:178–208.
[265] Fei J, Zhang J, Wang F, Wang J. Synergistic effects on co-pyrolysis of lignite and high-sulfur swelling coal. J Anal Appl Pyrol 2012;95:61–7.
[266] Knight J, Gorton C, Kovac R. Oil production by entrained flow pyrolysis of biomass. Biomass 1984;6:69–76.
[267] Maniatis K, Baeyens J, Peeters H, Roggeman G. The Egemin flash pyrolysis process: commissioning and initial results. Advances in thermochemical biomass conversion. Springer; 1993. p. 1257–64.
[268] Rüdiger H, Kicherer A, Greul U, Spliethoff H, Hein KR. Investigations in combined combustion of biomass and coal in power plant technology. Energy Fuels 1996;10:789–96.
[269] Storm C, Rüdiger H, Spliethoff H, Hein KR. Co-pyrolysis of coal/biomass and coal/sewage sludge mixtures. In: ASME 1998 international gas turbine and aeroengine congress and exhibition. American Society of Mechanical Engineers; 1998. p. V003T05A6-VT05A6.
[270] group Bt. Fast pyrolysis. 2020. 2020, https://www.btgworld.com/en/rtd/technologies/fast-pyrolysis. [Accessed 13 March 2020].
[271] Wehlte S, Meier D, Faix O. Wood waste management using flash pyrolysis in a fluidised bed. In: Proc frontiers of pyrolysis workshop. USA: Breckenridge, CO; 1995. June NREL.
[272] Knight J, Gorton C, Kovac R, Elston L, Hurst D. Oil production via entrained flow pyrolysis of biomass. In: Proceedings of the 13th biomass thermochemical conversion contractors' meeting, arlington, Virginia; 1981. p. 27–9.
[273] Papari S, Hawboldt K. A review on condensing system for biomass pyrolysis process. Fuel Process Technol 2018;180:1–13.
[274] Hu X, Gholizadeh M. Biomass pyrolysis: a review of the process development and challenges from initial researches up to the commercialisation stage. Journal of Energy Chemistry 2019;39:109–43.
[275] Perkins G, Bhaskar T, Konarova M. Process development status of fast pyrolysis technologies for the manufacture of renewable transport fuels from biomass. Renew Sustain Energy Rev 2018;90:292–315.
[276] Yun H, Clift R, Bi X. Process simulation, techno-economic evaluation and market analysis of supply chains for torrefied wood pellets from British Columbia: impacts of plant configuration and distance to market. Renew Sustain Energy Rev 2020;127:109745.